Developmental Cell
Review

Self-Organization in Pattern Formation

François Schweisguth[1,2,*] and Francis Corson[3,*]
[1]Institut Pasteur, Department of Developmental and Stem Cell Biology F-75015 Paris, France
[2]CNRS, UMR 3738 F-75015 Paris, France
[3]Laboratoire de Physique de l'Ecole Normale Supérieure, CNRS, Sorbonne Université, Université Paris Diderot 75005 Paris, France
*Correspondence: fschweis@pasteur.fr (F.S.), corson@lps.ens.fr (F.C.)
https://doi.org/10.1016/j.devcel.2019.05.019

Self-organization is pervasive in development, from symmetry breaking in the early embryo to tissue patterning and morphogenesis. For a few model systems, the underlying molecular and cellular processes are now sufficiently characterized that mathematical models can be confronted with experiments, to explore the dynamics of pattern formation. Here, we review selected systems, ranging from cyanobacteria to mammals, where different forms of cell-cell communication, acting alone or together with positional cues, drive the patterning of cell fates, highlighting the insights that even very simple models can provide as well as the challenges on the path to a predictive understanding of development.

Introduction

During development, an elaborate spatial structure is gradually established, through the allocation and spatial rearrangement of different cell types. Although much of development can be understood as a cascade of successive refinement steps, with early-formed landmarks providing positional cues for further subdivisions (Wolpert, 1969), some of these steps occur in the absence of overt positional cues, as in the development of the early mouse embryo (White et al., 2018). Self-organization is also evident in the ability of previously dissociated cells to recapitulate essential steps of development *in vitro*, from germ layer and axial patterning in cultures of mammalian stem cells (Beccari et al., 2018; Warmflash et al., 2014), to the development of organoids from cell aggregates (McCauley and Wells, 2017; Turner et al., 2016), to traveling waves of gene expression in cultures of presomitic mesoderm cells (Tsiairis and Aulehla, 2016). Self-organization, which may be defined broadly in the context of development as the spontaneous emergence of spatial order through cell-cell interactions, mediated e.g., by diffusing ligands or mechanical forces, can take different forms (Sasai, 2013). Here, we focus on self-organized tissue patterning, understood as the spontaneous patterning of cell fates. In this sense, self-organization is to be distinguished from self-assembly, as in the formation of epithelial structures such as tubules (Montesano et al., 1991) or somites (Dias et al., 2014), or the sorting of cells that have already acquired different fates through differences in cell adhesion or contractility (Fagotto, 2014); and from self-organized morphogenesis, which is not necessarily linked to fate patterning, as in the development of branched organs (Lu and Werb, 2008; Ochoa-Espinosa and Affolter, 2012), and in tissue buckling (Shyer et al., 2013). And while our focus is on the scale of the tissue, development can also involve self-organization within individual cells (Halatek et al., 2018), as in the polarization of the early *Caenorhabditis elegans* embryo (Goehring et al., 2011).

Principles and Models of Self-Organized Patterning

The dynamics brought about by mutual cell-cell interactions are difficult to anticipate and the experimental study of self-organization is inseparable from the exploration of mathematical models for pattern formation. Indeed, while some form of self-organization was implicit in the earlier concept of embryonic regulation (Roth, 2011), an explicit mechanism for spontaneous symmetry breaking—for the spontaneous generation of form—during development first came with the reaction-diffusion models introduced by Turing (Turing, 1952), in which cells interact through diffusing chemicals (Box 1). In a simple reaction-diffusion model, an activator stimulates its own production and the production of an inhibitor; if the inhibitor diffuses faster than the activator, a stable pattern can emerge from a uniform background through the amplification of small differences. In a two-dimensional geometry, which is a commonly adopted to reflect the geometry of tissues such as epithelia or skin, different choices of model parameters give rise to regular arrays of stripes or spots, which have notably been likened to animal coat patterns (Koch and Meinhardt, 1994; Murray, 2003). Beside stable patterns, reaction-diffusion models can also give rise to oscillations and traveling waves and have been proposed to describe somitogenesis (Cotterell et al., 2015). In addition to a large body of theoretical work (Koch and Meinhardt, 1994; Murray, 2003), Turing's ideas have stimulated the search for signaling molecules that could mediate pattern formation, and candidate activator-inhibitor pairs have been proposed to underlie patterning in diverse model systems, from hair and feather primordia (Michon et al., 2008; Sick et al., 2006) to palate rugae (Economou et al., 2012). Yet, as popular as the activator-inhibitor paradigm remains, models that are more closely tied to mechanism often require elaborations on this simple scenario, like the inclusion of nondiffusible species such as transcription factors, encoding a cell state that responds to signals and governs their production. And as Turing himself recognized, diffusing chemicals are just one way that cells can communicate. Long-range signaling can also be mediated by membrane-bound ligands carried by cellular projections, or by mechanical forces. Additionally, motile cells can arrange themselves into patterns of cell density, which may couple with cell fate. As mathematical models have explored, spontaneous cell aggregation can occur through secretion of an attractant (Keller and Segel, 1970), or

Box 1. Spontaneous Pattern Formation in Turing Models

In a Turing model, static cells interact through diffusing chemicals. Commonly, the diffusion ranges of the chemicals are taken to be larger than the scale of individual cells, and their interactions are described by partial differential equations for continuously varying concentrations. The simplest such model that supports patterning comprises two species. In the activator-inhibitor model (sketched below), self-activation of A competes with a stabilizing negative feedback through the inhibitor B. Equivalently, in a substrate-depletion model, negative feedback occurs through the consumption of a substrate that is required for the production of the activator. The equations for an activator-inhibitor model in one dimension can be written as

$$\begin{aligned} \partial_t A &= f_A(A,B) + D_A \partial_x^2 A, \\ \partial_t B &= f_B(A) - k_B B + D_B \partial_x^2 B, \end{aligned} \qquad \text{(Equation 1)}$$

where the functions f_A and f_B describe the interactions between A and B within each cell, D_A and D_B are their diffusion rates, and k_B stands for any negative feedback on B, e.g., constitutive degradation or self-inhibition.

One assumes that when the cells are uncoupled (in the absence of diffusion), negative feedback dominates, such that the tissue tends toward a stable state with uniform levels of the two chemicals. Nevertheless, in the presence of diffusion, it is possible for a pattern to spontaneously emerge through the amplification of small perturbations. In a linear stability analysis (Cross and Greenside, 2009; Murray, 2003), the time evolution of a perturbation is approximated by a linear equation, e.g., for the activator-inhibitor model

$$\begin{aligned} \partial_t A &= \alpha A - \beta B + D_A \partial_x^2 A, \\ \partial_t B &= A - k_B B + D_B \partial_x^2 B, \end{aligned} \qquad \text{(Equation 2)}$$

where A and B now denote the deviation from the unperturbed state. Diffusion is irrelevant (stability is unaffected by coupling) on the largest spatial scales and dampens small-scale perturbations. Perturbations at intermediate length scales, on the other hand, can grow, provided that the inhibitor has a greater diffusion length than the activator, where the diffusion lengths l_A and l_B are given by $l_A^2 = D_A/\alpha$ and $l_B^2 = D_B/k_B$ (Cross and Greenside, 2009). Intuitively, at length scales that are larger than l_A but smaller than l_B, variations in inhibitor level are damped, thus self-inhibition is reduced, while self-activation of A is preserved. Because stability in the absence of diffusion requires $k_B > \alpha$, the above condition on diffusion lengths implies the condition that is most commonly associated with patterning in Turing models, that the diffusivity of the inhibitor is larger than that of the activator. The latter condition is more practical since the diffusivities are experimentally accessible physical parameters, whereas the "diffusion length" l_A involves the regulation of A.

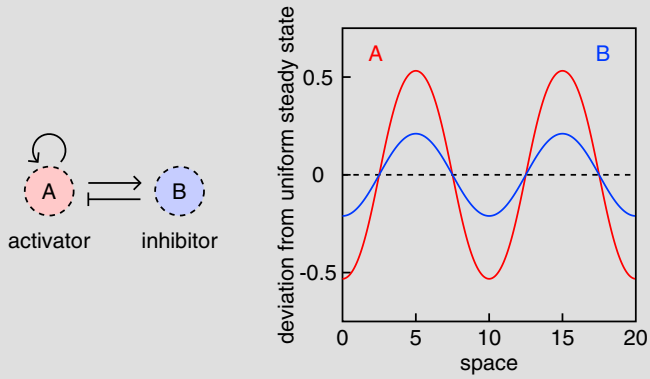

Starting from a uniform background, amplification of perturbations leads to a periodic pattern, with a spatial scale that is typically set by the fastest growing perturbation (other outcomes are possible, which include traveling waves in models with at least three species, but steady waves are most relevant here). In a one-dimensional system, the resulting patterns show a regular alternation of high and low activator levels (the figure above shows a pattern obtained with the parameter values $\alpha = \beta = k_B = D_A = 1$ and $D_B = 4$, such that $l_A = 1$ and $l_B = 2$, and with a stabilizing term $-A^3$ added to the equation for A to produce a finite-amplitude pattern). In two dimensions, generic outcomes include stripes and spots. In a weakly nonlinear analysis (in the regime close to the instability threshold, where the amplitude of the pattern is small), the pattern is described as a superposition of waves of different orientations, e.g., the overlap between three stripe patterns at 120° angles forms a hexagonal array of spots. Such an analysis suggests that if the system is symmetric with respect to the sign of the perturbation, stripes are selected, whereas an asymmetry favors spots (Cross and Greenside, 2009; Ermentrout, 1991). Intuitively, in the symmetric case there are equal areas of high and low activator, and they will be arranged in stripes. If we consider instead an asymmetric case, e.g., a faster than linear increase

(Continued on next page)

Box 1. *Continued*

in inhibitor vs. activator level, the balance between activation and inhibition shifts as the perturbation grows, yielding a smaller activated region, arranged in spots.

Of note, Turing models as described above involve several idealizations. For instance, tissue that is truly three-dimensional is commonly described in two-dimensions. While the geometry of the tissues of interest, such as epithelia or skin, make this a reasonable simplification, it is also possible that exchange of signaling molecules with the surrounding medium may contribute to their apparent degradation rate, and/or to their transport. In some cases, like angelfish stripes (Kondo and Asal, 1995), the geometry of the pattern may motivate a one-dimensional model, yet the stability of the same pattern in a two-dimensional setting should be considered (Höfer and Maini, 1996). In addition, what appears as simple diffusion in the models reflects complex transport processes, that may be affected by the tortuosity of the intercellular space, and hindered or facilitated through binding with immobilized molecules or shuttles, and whose regulation in space and time may play important roles in patterning (Akiyama and Gibson, 2015; Müller et al., 2013).

DISCRETE MODELS

Models that explicitly incorporate discrete cells are required in some contexts, such as the emergence of salt-and-pepper patterns through lateral inhibition. In a discrete model, ordinary differential equations describe the evolution of concentrations in individual cells. Generally, these models lend themselves to the same mathematical treatment, e.g., linear stability analysis, as continuous models (Plahte, 2001). All the while, they exhibit some specific features: whereas some form of short-range positive feedback, or diffusion, is required to maintain smooth concentration profiles in continuous models, cell-intrinsic positive feedback (e.g., gene self-activation) and a single, inhibitory signal can support the emergence of a discrete pattern (below left). This can be likened to an activator-inhibitor model where the scale of the pattern tends to the scale of a cell and could describe the early stages of heterocyst patterning in Anabaena (cf. Figure 1). In the specific case of paracrine signaling, as in Notch-mediated lateral inhibition, an inhibitor alone is sufficient for patterning. In the absence of self-inhibition, cell-intrinsic positive feedback is not required. Instead, mutual inhibition between neighboring cells acts as a double-negative feedback loop, amplifying differences between cells (below right) (Collier et al., 1996).

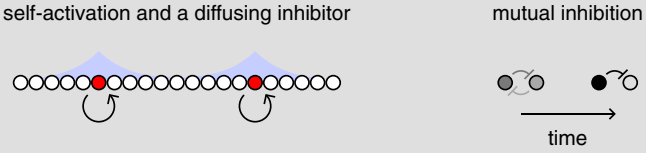

through mechanical cues transmitted by the extracellular matrix (Murray et al., 1983). Although, strictly speaking, Turing models involve interactions based on diffusing chemicals, it is noteworthy that models assuming different forms of cell-cell communication can be very similar in their mathematical structure and patterning behavior. And to some extent, different interaction modalities can be subsumed under a generic "interaction function" (Hiscock and Megason, 2015) (Box 2), which could provide a common framework to address the logic of pattern-forming systems. For instance, pattern-forming models commonly involve local activation and long-range inhibition, but as we discuss below, whether this must always be the case remains a matter of debate.

In addition to involving different forms of interactions, self-organized patterning can give rise to different forms of spatial structure. As a general rule, the range of cell-cell interactions, e.g., the diffusion range of signaling molecules, governs the size of pattern elements, determining different classes of patterns and calling for different modeling approaches. Long-ranged interactions give rise to smoothly varying patterns of signaling activity and gene expression, at least before a stage where fate boundaries sharpen, and the relevant variables are commonly described as continuously varying functions of space. Short-ranged interactions, by contrast, can form patterns of isolated cells, like the salt-and-pepper arrangements of neural cells arising through lateral inhibition, and call for models that explicitly describe individual cells. Depending on how the range of interactions compares to the size of the tissue, the output of self-organization can range from tissue-wide gradients, defining a positional cue for downstream patterning events, as in left-right patterning in the mouse (Nakamura et al., 2006), to patterns comprised of a small, invariant number of elements, such as digits in mammals (Raspopovic et al., 2014) and stripes in fishes (Nakamasu et al., 2009), to a uniform covering with regularly spaced elements, such as hair and feather primordia (Michon et al., 2008; Sick et al., 2006).

Self-organized patterning is commonly contrasted with the specification of cell fates by positional cues, yet it is likely that much of development involves an interplay between pre-existing cues and cell-cell interactions, more than one or the other (Green and Sharpe, 2015). Purely self-organized patterns, arising from initial or temporal fluctuations, are by essence variable, and models for disordered patterns such as hair primordia can compare with experiment only in an average sense, judging e.g., by the typical size or spacing of pattern elements in control or perturbed conditions. However, where the output is a

Box 2. The Notion of Interaction Function

The activator-inhibitor model, The simplicity of the model, and its relatively intuitive behavior, balancing local activation and long-range inhibition, explain its appeal. Yet most patterning processes involve multiple signaling pathways, and an interplay between diffusing molecules, such as extracellular ligands, and cell-bound species, such as cell surface receptors and transcription factors. Models that explicitly account for this complexity are less straightforward to analyze systematically, and whether they lend themselves to an intuitive interpretation is unclear. The notion of "interaction function" (Hiscock and Megason, 2015) may provide an element of answer.

As a simple example, consider a model with one immobile species, e.g., a transcription factor, C, and a diffusible activator-inhibitor pair, A, B (see sketch below; dashed circles denote diffusing species), described by the following equations:

$$\begin{aligned} \partial_t A &= f_A(C) - k_A A + D_A \partial_x^2 A, \\ \partial_t B &= f_B(C) - k_B B + D_B \partial_x^2 B, \\ \partial_t C &= f_C(A, B, C). \end{aligned} \qquad \text{(Equation 3)}$$

This is logically equivalent to the model of (Raspopovic et al., 2014) for digit patterning, if one associates high C with the interdigit fate (low Sox9; cf. Figure 2). The linearized equations for a small perturbation are of the form

$$\begin{aligned} \partial_t A &= C - k_A A + D_A \partial_x^2 A, \\ \partial_t B &= C - k_B B + D_B \partial_x^2 B, \\ \partial_t C &= \alpha A - \beta B + \gamma C, \end{aligned} \qquad \text{(Equation 4)}$$

where, as in Box 1, we use the same notation, A, B, C, to denote the perturbation, for simplicity.

The analysis is greatly simplified, and the patterning behavior of the model becomes more transparent, if one considers a regime where the diffusing signals are close to a steady-state profile, with production, diffusion, and degradation balanced. This approximation is justified when the system is marginally unstable and the pattern develops slowly. In that limit, signaling is effectively instantaneous, and can be subsumed under an interaction function that couples the dynamics of the immobile species C at different positions (in different cells). For a one-dimensional system or perturbation, a cell at position X gives rise to a signaling field with profiles of A and B that decay exponentially with the distance x-X

$$\begin{aligned} K_A(x - X) &= \frac{1}{2k_A l_A} e^{-\frac{|x-X|}{l_A}}, \\ K_B(x - X) &= \frac{1}{2k_B l_B} e^{-\frac{|x-X|}{l_B}}, \end{aligned} \qquad \text{(Equation 5)}$$

per unit of C in the cell (see plots below); l_A and l_B are the diffusion ranges of the activator and inhibitor, $l_A^2 = D_A/k_A$ and $l_B^2 = D_B/k_B$. Summing over all the cells (integrating over X) and inserting into the equation for C (Equation 4) allows the dynamics to be expressed in terms of the immobile species alone,

$$\partial_t C(x) = \gamma C(x) + \int K(x - X) C(X) dX. \qquad \text{(Equation 6)}$$

In this equation, the influence of a cell at position X on a cell at position x it captured by the interaction function (plotted below)

$$K(x - X) = \alpha K_A(x - X) + \beta K_B(x - X) = \frac{\alpha}{2k_A l_A} e^{-\frac{|x-X|}{l_A}} - \frac{\beta}{2k_B l_B} e^{-\frac{|x-X|}{l_B}}. \qquad \text{(Equation 7)}$$

Equations of this form, which could equally describe signaling mediated by cellular projections, have also been considered to describe patterns of activity in neural fields (Amari, 1977). Analysis of Equation 6 shows that patterning requires $l_B > l_A$, i.e., a greater diffusion range of the inhibitor. Of note, stability toward small-scale perturbations, and a smooth pattern, require that cell-intrinsic dynamics be stabilizing, i.e., $\gamma < 0$; the digit model of (Raspopovic et al., 2014) corresponds to the marginal case $\gamma = 0$, and yields a singular Sox9 profile, with an infinite slope at the digit-interdigit boundary (see Figure 2C).

The right-hand plot below shows a pattern obtained with the parameter values $\alpha = \beta = 1/4$, $\gamma = -.05$, $k_A = k_B = D_A = 1$, and $D_B = 4$, such that $l_A = 1$ and $l_B = 2$, and with a stabilizing term $-C^3$ added to equation for C; the magenta curve shows the interaction term $\alpha A - \beta B$ appearing in that equation.

(Continued on next page)

Box 2. *Continued*

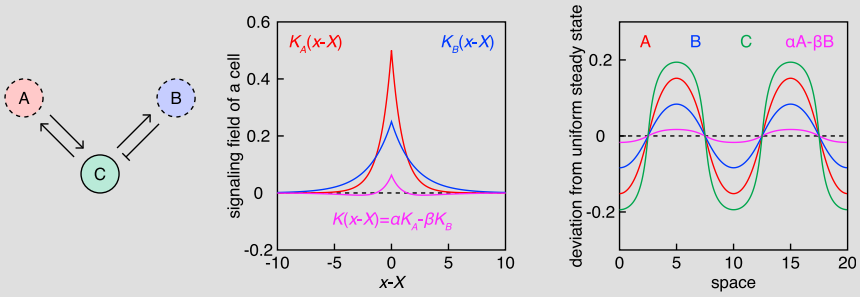

Interaction functions can also be defined for motile cells (Hiscock and Megason, 2015), with model variables now including cell densities. In addition, different networks of interactions can give rise to qualitatively similar interaction functions. As a specific example, the interaction function for the network represented below, from (Marcon et al., 2016), has the same form as for the network shown above, i.e.,

$$K(x) = \frac{\alpha}{2k_A l_A} e^{-\frac{|x|}{l_A}} - \frac{\beta}{2k_A k_B} \frac{l_A e^{-\frac{|x|}{l_A}} - l_B e^{-\frac{|x|}{l_B}}}{l_A^2 - l_B^2}. \qquad \text{(Equation 8)}$$

The same profile, with short-range positive feedback and long-range negative feedback, can be recovered with the diffusion ranges of the activator and inhibitor being swapped, as illustrated below (here, $\alpha = \beta = 3/4$, $D_A = 4$ and $D_B = 1$, such that $l_A = 2$ and $l_B = 1$; other parameter values are the same as above; notice that A and B have different profiles, but the same interaction function and the same interaction term $\alpha A - \beta B$ are recovered).

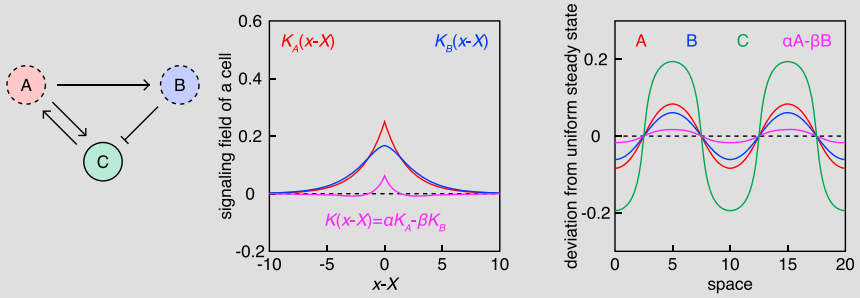

As an implication, experiments that probe the effective interaction between cells may not be sufficient to discriminate between candidate networks. On the other hand, if enough information is obtained on the structure of the interaction function (e.g., by relating gene expression and signaling activity patterns), is may be possible to describe the dynamics of patterning without a comprehensive characterization of molecular interactions. Taken together, interaction functions may provide a unifying framework to analyze seemingly disparate patterning models.

stereotyped arrangement like digits in mammals (Raspopovic et al., 2014), or a gradient with an invariant orientation, like Nodal in zebrafish (Müller et al., 2012), it must be that particular initial or boundary conditions steer patterning toward a reproducible outcome. Such a bias may arise from pre-existing positional cues, or from the geometry of the tissue itself, possibly including its growth. Reaction-diffusion models that would generically produce variable outcomes follow a determined sequence in a growing domain (Crampin et al., 1999) and the borders of stem cell colonies grown on patterned substrates, acting as sinks for diffusing ligands, have been proposed to provide a positional cue for stereotyped radial patterning (Etoc et al., 2016). Such a role for initial or boundary conditions is not restricted to patterns of a few elements, since large-scale patterns that are constrained to form sequentially can exhibit long-range order, like the arrangement of ommatidia in the *Drosophila* eye, which forms in the wake of a traveling differentiation front (Lubensky et al., 2011; Roignant and Treisman, 2009), or the arrangement of feathers in chick (Ho et al., 2019). And in the same way that self-organized patterns never emerge on a perfectly blank slate, there is much evidence to suggest that cell-cell interactions can refine the interpretation of morphogen gradients, or even that the receiving cells contribute to shaping the gradient, as in the patterning of the vertebrate neural tube by Sonic Hedgehog (Shh) (Ribes and Briscoe, 2009). The establishment of gradients of Nodal and its inhibitor Lefty in the zebrafish embryo is one rare example where molecular diffusivities were quantified and supported a Turing model (Müller et al., 2012), yet recent

experiments suggest that inhibitory feedback from Lefty is not strictly required for patterning, since uniform Lefty expression rescued lefty mutants (Rogers et al., 2017)—thus many gradient-forming systems may exist on a continuum between positional information and self-organized patterning.

As this overview should make clear, self-organized patterning encompasses very diverse phenomena and model systems. Rather than aim for a comprehensive survey, we have chosen to focus primarily on patterns of repeated elements and on a few experimental settings in which experimental data can now be confronted with models in a semiquantitative manner, ranging from a simple one-dimensional system in prokaryotes to the more complex two-dimensional pattern of the lizard skin. For reasons of space, many other systems of interest are not covered here, including the establishment of tissue-wide gradients in vertebrates through Nodal and Lefty (Müller et al., 2012; Nakamura et al., 2006) and during planarian regeneration (Stückemann et al., 2017), somitogenesis (Hubaud et al., 2017; Pourquié, 2011; Sonnen et al., 2018), and patterning in plants (Bhatia and Heisler, 2018). Self-organized patterning in the early mammalian embryo has been covered in a separate review (White et al., 2018). The systems covered here illustrate various forms of cell-cell communication, from diffusing ligands to mechanical forces, different modeling approaches, from continuous to cell-based, and various forms of interplay between positional cues and self-organization. As these examples also illustrate, and as we further discuss in closing, self-organized patterning often involves an interplay between multiple signals, whether chemical or mechanical, of which a subset may suffice to explain the observed outcome. While such an apparent redundancy can be rationalized as a conferring robustness on development, it implies that striking a balance between model complexity, predictive power, and interpretability is a delicate exercise, and that proving or disproving any particular mechanism may require stringent tests, beyond assessing the effect of uniform perturbations on the final pattern.

A One-Dimensional Self-Organizing System in Cyanobacteria

A comparatively simple instance of a self-organized pattern is observed in several species of cyanobacteria such as *Anabaena*, which form colonies consisting of one-dimensional filaments with a periodic pattern of two distinct cell types (Kumar et al., 2010; Meeks and Elhai, 2002; Wilcox et al., 1973a; 1973b). In the presence of nitrogen sources, the filaments comprise only mitotically active vegetative cells that carry photosynthesis. In contrast, under nitrogen-limiting conditions, some cells stop dividing and differentiate into heterocysts that can fix atmospheric nitrogen. A key feature of this system is that heterocysts appear at regular intervals, forming a one-dimensional pattern of heterocysts separated by about ten vegetative cells. This pattern is dynamic: as vegetative cells continue to divide, new heterocysts differentiate in the middle of the intervals between pre-existing heterocysts, so that a regular pattern is maintained over time.

This basic phenomenology suggested that lateral inhibition from differentiated heterocysts maintains a regular spacing pattern. An early mathematical model that postulated a diffusing inhibitor, with an exponential decay away from heterocysts, agreed well with the measured distribution of intervals between the first-formed heterocysts (Wilcox et al., 1973a; Wolk and Quine, 1975). Subsequent experimental studies provided support for this model. Heterocyst differentiation is positively regulated by a transcription factor, HetR, that is inhibited by two short diffusible peptides, HetN and PatS that inhibit HetR (Corrales-Guerrero et al., 2013; Kumar et al., 2010; Risser and Callahan, 2009). While HetR and PatS display basal fluctuating levels under nitrogen-rich conditions (HetN only appears later in differentiated heterocysts and acts mostly in pattern maintenance) (Corrales-Guerrero et al., 2015), an upstream regulator of HetR is activated upon nitrogen stress and elevated levels of HetR in turn up-regulate PatS expression (Figure 1).

The identification of these molecular players, and the resulting mathematical models (Brown and Rutenberg, 2014; Muñoz-García and Ares, 2016) have provided a clearer picture of patterning in cyanobacteria. Yet they leave some intriguing features of heterocyst differentiation unexplained. Early observations suggested that differentiating heterocysts do not emerge in isolation, as could be expected from a simple lateral inhibition mechanism. Rather, strings of differentiating cells are often observed, that later resolve- into a single heterocyst (Wilcox et al., 1973a) (see also the pattern of HetR expression in Figure 1A). This suggested a "two-stage" model, where differentiation is first initiated in groups of competent cells, followed by their resolution (Corrales-Guerrero et al., 2015; Meeks and Elhai, 2002). The emergence of the groups at regular intervals may suggest spatially correlated fluctuations in the basal expression of HetR. Indeed, live imaging of a HetR-GFP fusion protein and analysis of spatial fluctuations under nitrogen-rich conditions suggest coupling between neighboring cells (Corrales-Guerrero et al., 2015). Alternatively, spatially correlated cell cycle phases, on a scale commensurate with the heterocyst pattern (Meeks and Elhai, 2002), and asymmetries arising through division in protein content (Risser et al., 2012) or cell size (Mitchison and Wilcox, 1972), might modulate cell competence. When most mathematical studies of pattern formation emphasize the selective amplification of random fluctuations as the main driver of pattern selection, the example of *Anabaena* thus points to the possible role of pre-existing structure within a population of equivalent cells. Such a pre-existing bias, resulting from a difference in birth order, has been proposed to underlie the AC/VU decision in *C. elegans* (Karp and Greenwald, 2003). In cyanobacteria, structured fluctuations on scales large and small could facilitate symmetry breaking in the two stages of patterning. Live imaging along with mathematical models that explicitly integrate correlated fluctuations should reveal how pattering builds on a structured background.

Also, can one rationalize the existence of two diffusing inhibitors, HetN and PatS, where one might seem enough to support the emergence of the pattern and its maintenance during growth? Could it be that heterocyst selection among competent cells calls for a fast inhibitor turnover, while an inhibitor with a slower turnover can support lateral inhibition from differentiated heterocysts at a reduced "cost"? Or does the transition from mutual to lateral inhibition require a subtle regulation of inhibitor levels, that is more "readily" achieved by combining multiple inhibitors, with individually simpler regulation? By formalizing such questions, modeling could help define further experiments

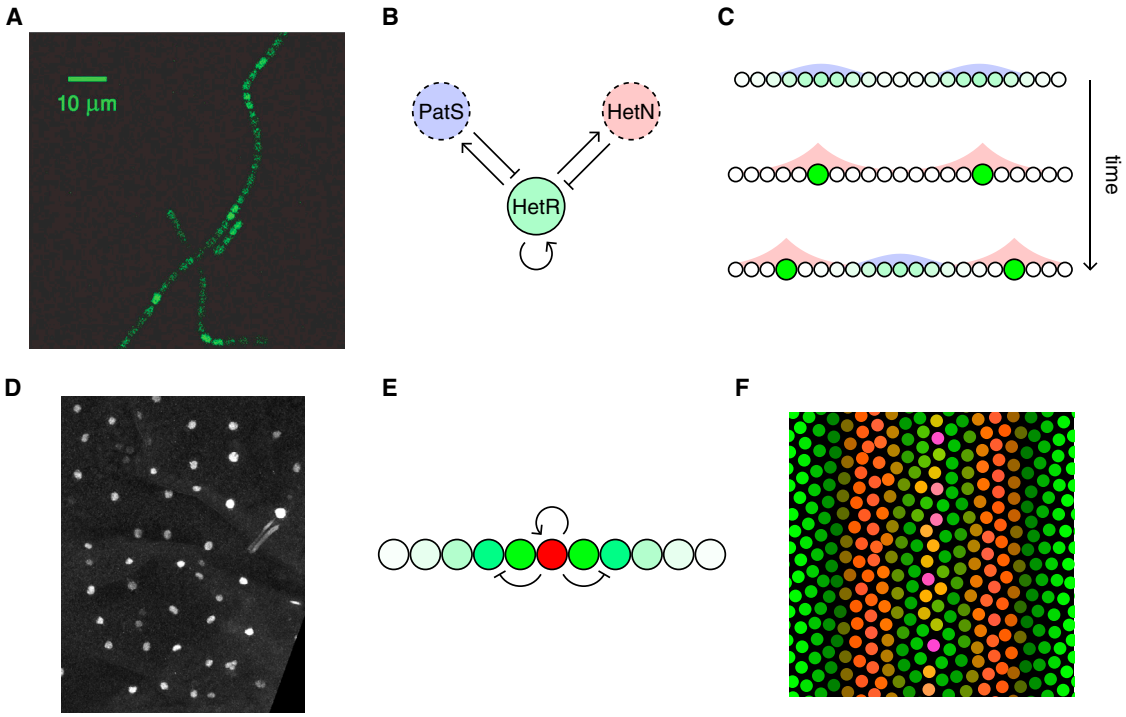

Figure 1. Lateral Inhibition Patterning in One and Two Dimensions

(A–C) Heterocyst patterning in nitrogen-deprived cyanobacteria.

(A) Expression of HetR-GFP in differentiating heterocysts in *Anabaena*, 7 h after nitrogen step-down (from Corrales-Guerrero et al. [2015]). Notice the elevated HetR-GFP expression in groups of adjacent cells.

(B) Heterocyst patterning involves the self-activating transcription factor HetR, and lateral inhibition mediated by two short diffusible peptides, PatS and HetN.

(C) Following nitrogen deprivation, HetR-expressing heterocysts (green) are selected through PatS-mediated lateral inhibition (blue). Inhibition around differentiated heterocysts is later sustained by HetN (red). During subsequent growth of the filament, new heterocysts intercalate between existing ones, maintaining a regular spacing.

(D–F) Sensory organ patterning in the *Drosophila* thorax.

(D) In the pupal thorax, sensory organ precursors (SOPs, labeled by expression of the transcription factor Sensless) that give rise to bristles in the adult fly are arranged in regular rows.

(E and F) A simple mathematical model, with a single variable per cell standing for proneural activity (red), recapitulates SOP patterning. The model incorporates self-activation and Notch-mediated lateral inhibition (green). With boundary conditions that mimic early Notch activity in the thorax, the model produces a sequence of proneural stripes that resolve into SOP rows, as observed (adapted from Corson et al. [2017]).

to dissect the regulatory architecture underlying the formation and maintenance of a regular spacing pattern in cyanobacteria.

Stripes and Dots: Self-Organization in Flies

While patterning in cyanobacteria affords a simple example of a one-dimensional spacing pattern, the suggestion that such arrangements arise from lateral inhibition first arose from the study of sensory organ patterns on the epidermis of insects, and Wigglesworth's observations on the development of sensory bristles in the blood-sucking bug *Rhodnius*. *Rhodnius* grows in size through five nymphal stages, with new sensory bristles emerging at each molt. Noting that these new bristles develop in the largest intervals between existing ones, Wigglesworth proposed that bristles exert an inhibitory influence on their surroundings, possibly by consuming a uniformly produced bristle-promoting factor (Wigglesworth, 1940), as in a substrate-depletion model (see Box 1). A regular spacing pattern would thus be maintained as the body enlarges. Four decades later, genetic and molecular studies in *Drosophila* led to revisit this model. In contrast with *Rhodnius*, the adult fly is produced at once to its final size by the differentiation of imaginal tissues through a complete metamorphosis, thus bristles develop in their definitive pattern, without subsequent insertion of new bristles. Where bristles can form is governed by the expression of proneural transcription factors such as Achaete and Scute, which endow cells with the competence to become sensory organ precursor cells (SOPs). SOPs are then selected from among the competent cells through lateral inhibition mediated by Delta ligand and Notch receptor (Ghysen and Dambly-Chaudière, 1989; Simpson, 1990), which antagonizes the activity and expression of the proneural factors through its E(spl)-HLH targets (Delidakis et al., 2014). The pattern of proneural gene expression thus largely prefigures the layout of sensory organs (Campuzano and Modolell, 1992). In some places, a fixed number of large sensory bristles develop at invariant locations, and this was traced to the activity of specific *cis-regulatory* enhancers in the *Achate-Scute Complex* locus that integrate positional cues and direct proneural expression in small clusters of cells (Gómez-Skarmeta et al., 2003). Here, Notch-mediated cell-cell interactions are understood to simply refine the readout of positional cues. As a caveat, this model does not readily account for the emergence of SOPs near the center of proneural clusters, where

inhibition is expected to be strongest, unless one assumes a sharp spatial bias that favors a subgroup of cells (Troost et al., 2015). In broad regions of competence, by contrast, lateral inhibition should produce irregular arrays of isolated SOPs. Indeed, some areas of the body are covered with irregular arrangements of small bristles. Such "salt-and-pepper" patterns arise in mathematical models of lateral inhibition patterning, centered on the dynamics of Notch and Delta, through the amplification of small differences between cells (Collier et al., 1996; Heitzler and Simpson, 1991). Of note, these models, by contrast with models of heterocyst patterning in cyanobacteria, do not require cell-autonomous positive feedback, since signaling is restricted to a cell's neighbors and there is no self-inhibition. In other areas of the body, however, extended arrays of bristles exhibit regular arrangements. In the medial thorax, for instance, five rows of bristles develop on each side of the midline (see the SOP pattern in Figure 1D). Each of these rows emerges from a proneural stripe that could reflect an underlying prepattern. It appears, however that these stripes are not individually specified by specific enhancers of the *achaete* and *scute* genes (Corson et al., 2017). Instead, they develop in a defined temporal sequence that is suggestive of a self-organized process. Supporting this view, analysis of proneural and Notch activity over the course of patterning revealed that this sequence is governed by Notch signaling. Before proneural genes are expressed, a bimodal gradient of Delta gives rise to two bands of Notch activity in regions of intermediate Delta levels, forming a negative template for the expression of Achaete and Scute in stripes 1, 3, and 5 (Corson et al., 2017). Concomitant with the onset of Achaete and Scute expression in these first three stripes, Delta is expressed in stripe 3 and Notch activity becomes dynamic. This expression of Delta does not depend on Achaete and Scute (Parks et al., 1997), suggesting that Notch independently serves as a negative template for the expression of Delta. As the first three stripes begin to resolve, two bands of low Notch activity appear between them, allowing the emergence of stripes 2 and 4. Within each stripe, proneural activity is initially higher in the center that on the sides, and SOPs are eventually selected from the more central cells, producing rows of regularly spaced SOPs. These observations suggested that in the medial thorax, Notch signaling governs both proneural patterning and SOP selection—a suggestion that was supported by a simple model for Notch-mediated patterning (Figures 1E and 1F). This minimal model, with a single scalar variable for the state of each cell, describes how cell states vary according to inhibitory signaling activity; signal production is a function of cell state and propagation is instantaneous. Simulated in a two-dimensional field of cells, with an initial pattern of signaling activity that mimics the early Delta gradient, the model recapitulated the sequential emergence of stripes and their resolution (Corson et al., 2017). The model further suggested that cell-intrinsic positive feedback, although not strictly required for lateral inhibition patterning, accounts for the emergence of SOPs at the center of the stripes. Such feedback, which could result from proneural self-activation and/or Notch *cis*-inhibition, and which gives rise to a bistable response, allows cells with higher proneural activity to evade inhibition, even though they are exposed to higher Delta levels. The model also required a nonlinear progression of signal production as a function of cell state, which could result from the action of signaling modulators such as Neuralized and shapes the transition from mutual inhibition among proneural cells to lateral inhibition from SOPs (Corson et al., 2017). With these ingredients, the model encapsulates the multistep process of proneural cluster resolution that was proposed earlier (Troost et al., 2015), with no need for specific mechanisms to restrict competence to a subgroup of cells or preselect SOPs; instead, the interplay between cell-intrinsic dynamics and signaling drives a gradual refinement of cell fates.

Taken together, model and experiments indicated that positional cues (a gradient of Delta that is decoded through *cis*-inhibition and transactivation) and cell-cell interactions combine to create a regular pattern of proneural stripes and bristle rows (Corson et al., 2017). In other tissues, different spatial or temporal cues impinging on lateral inhibition patterning may give rise to different cell fate arrangements. In the *Drosophila* eye, for instance, patterning along a traveling differentiation front produces a regular array of R8 photoreceptors, arranged in a hexagonal lattice (Lubensky et al., 2011; Roignant and Treisman, 2009). While the overall logic of bristle patterning is clear, some issues remain open. For instance, how inhibitory signaling extends beyond immediate neighbors, as required in the model to account for the observed SOP spacing, remains to be established: although long-range signaling may involve basal filopodia (Cohen et al., 2010; De Joussineau et al., 2003), direct experimental evidence for Delta signaling at basal filopodia is still lacking. Also, while Notch *cis*-inhibition (del Álamo et al., 2011) has been proposed to yield a sharper segregation of cell fates (Barad et al., 2010; Sprinzak et al., 2011), whether *cis*-inhibition actually contributes to SOP selection remains to be tested. In summary, a self-organized process guided by temporal and spatial, or boundary, cues orchestrates the patterning of sensory organs in the dorsal thorax of *Drosophila* (Corson et al., 2017). In this context, the number of bristles per row varies between animals, and with the size of the field. By contrast, variability in the number of rows is much more limited, e.g., starved flies can partially miss a late-appearing row whereas well-fed overgrown flies can exhibit an extra row (Simpson et al., 1999). In other words, this self-organized process results in a stereotyped outcome that is relatively insensitive to physiological perturbations and genetic variation. Self-organization guided by stereotyped initial and/or boundary conditions may thus be a path to reproducible outcomes during development.

A Turing System for Digit Patterning in Tetrapods

While discrete spacing patterns arising through cell-intrinsic positive feedback and lateral inhibition can be conceived as a limiting case of Turing models, these are more commonly associated with the specification of larger-scale elements. In particular, reaction-diffusion models have been proposed to underlie the development of various body structures in vertebrates, including digits in tetrapods (Cooper, 2015) and ridges on the palate of mammals (Economou et al., 2012; Lan et al., 2015). The idea that reaction-diffusion may account for the patterning of skeletal elements in developing limbs dates back to the 1970s (Cooper, 2015; Newman and Frisch, 1979; Wilby and Ede, 1975). Since then, experiments in chick and mouse have provided a detailed view of the molecular and cellular processes that direct the digit versus interdigit decision, which now allow

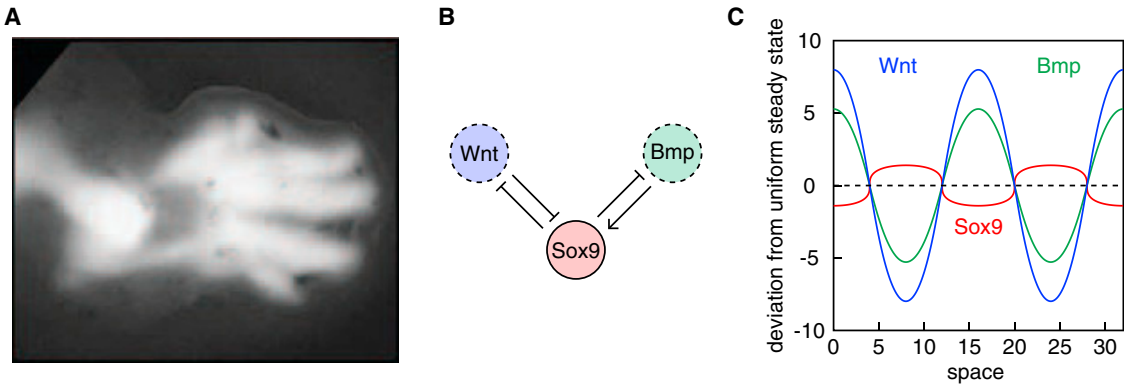

Figure 2. A Turing Model for Digit Patterning in Vertebrates
(A) Expression of Sox9-EGFP marks digits in limb culture (from Raspopovic et al. [2014]).
(B) A proposed Turing network for limb patterning, comprised of the transcription factor Sox9 and two diffusing species, Wnt and Bmp.
(C) Simulated in one dimension, the model gives rise to patterns in which regions of high Sox9 alternate with regions of high Wnt and Bmp [after (Raspopovic et al., 2014)].

theory to be more explicitly confronted with experiments (Miura and Shiota, 2000; Onimaru et al., 2016; Raspopovic et al., 2014; Sheth et al., 2012).

Vertebrate limbs appear as small buds produced by the epithelial-to-mesenchymal transition of trunk epithelial cells at specific locations along the body (Gros and Tabin, 2014). These buds produce a small number of digits, e.g., three in the chick forelimb and five in mouse limbs, which are morphologically distinct along the anterior-posterior (a-p) axis. Classical grafting experiments indicated that positional information, in the form of a Shh gradient, instructs the morphological identity of digits (but see also Delgado and Torres, (2016) for a review of the experimental evidence challenging this view). While in principle positional information could be interpreted to generate a periodic pattern, mutations in components of the Shh signaling pathway result in polydactyly because of an increase in cell proliferation and a larger limb (Towers et al., 2008; Zhu et al., 2008) rather than in altered periodicity of the pattern. This indicates that Shh regulates the size of the digit field but is not required for digit patterning per se. Moreover, loss of positional identity, through dissociation, reaggregation and grafting of limb cells, does not block digit formation (Zwilling, 1964). Thus, generating digits and specifying morphological identities are largely independent processes.

The idea that digit patterning is self-organized, and might be described by a reaction-diffusion model, is supported by several observations. First, time-course analysis of the emergence of digit condensations in the developing limb indicates that digits appear as regularly spaced condensations in a defined temporal order as the digit field grows (Hiscock et al., 2017; Raspopovic et al., 2014; Zhu et al., 2008). Second, an allelic series of mutations in the *Hoxa13*, *Hoxd11-13*, and *Gli3* genes produces mouse mutant embryos with a gradual increase in digit number, ranging from five up to thirteen. While this phenotype may reflect the changing wavelength of a Turing-like pattern of stripes (Sheth et al., 2012), the observation that digits may be initiated as spots and extend with growth, rather than being specified *de novo* as stripes (Hiscock et al., 2017), suggested a different interpretation of these phenotypes: spots develop with the same spacing along the a–p axis but at a more distal position within the limb, where the digit field is broader (Hiscock et al., 2017). In this view, digits appear at regular intervals and their number is defined by the size of the digit field, as a Turing-like system would predict (Hiscock et al., 2017). Third, using Sox9 as an early digit marker, dissociated limb cells could form periodic patterns *ex vivo* (Raspopovic et al., 2014) (see also [Miura and Shiota, 2000; Ros et al., 1994]). Together, these data support the view that a Turing-like system may be at play.

What then is the molecular dynamics underlying this patterning system? A transcription factor, Sox9, and two signals, BMP and Wnt, were recently proposed to be part of a three-node Turing system (Figure 2) (Raspopovic et al., 2014). Indeed, Sox9 expression, marking the future digits, is in phase with BMP activity (phosphorylated Smad) but out of phase with Wnt signaling activity (β-catenin). Loss and/or inhibition of Sox9, BMP, and Wnt activities disrupt patterning with BMP activating and Wnt repressing Sox9 expression (Akiyama et al., 2002; Raspopovic et al., 2014). Absent a full characterization of the interactions between Sox9, BMP, and Wnt, an exploration of possible network structures identified a minimal topology that could support digit patterning. In a fixed domain and with uniform parameters, the model produces labyrinthine patterns, but with suitable conditions, incorporating growth of the limb and plausible proximo-distal gradients of its parameters, it recapitulates the sequence of digit formation, as seen in patterns of Sox9 expression. Consistent with the model, combined inhibition of BMP (digit loss) and Wnt (interdigit loss) resulted in fewer and larger digits (Raspopovic et al., 2014). In addition, the expression and function of Sox9, BMP, and Wnt appear to be conserved for the skeletal patterning in the fins of fishes (Onimaru et al., 2016). Nevertheless, some questions remain unanswered. First, since none of the Wnt ligands is known to be expressed in a periodic manner, it is not clear how Wnt signaling is spatially restricted. Second, BMP activity (phosphorylated Smad) and Bmp2 expression, which are subsumed under the same variable in the three-node model, are actually out of phase. While this observation could be explained by a more complex model, in which Wnt downregulates phosphorylated Smad downstream of BMP (Marcon et al., 2016), whether and how this interaction occurs remains to be ascertained.

Taken together, the published evidence makes a compelling case that digit patterning involves a Turing-like system, yet the precise nature of the relevant interactions, and their molecular basis, remains to be clarified. Also, more stringent tests of the model would be desirable. Indeed, while the proposed model matches the data, the latter do not necessarily exclude other models, e.g., cell-based models such as cell mobility toward cartilage-like condensations (discussed in Hiscock and Megason, 2015). If digits appear as spot-like condensations, the temporal order of emergence of these spots should be revealing. Thus, further tests of the simple three-node Turing model (Raspopovic et al., 2014) and of its more realistic five-node version (Marcon et al., 2016) may require an analysis of the dynamics of spot emergence upon experimental perturbations predicted to affect the number, size, and/or spacing of these spots. In the future, combining endogenous GFP-tagged signaling molecules and activity reporters with *ex vivo* live imaging should permit to confront the model with experimental data in a quantitative manner.

Conditions for Patterning in Mathematical Models

The example of digit patterning, like other systems involving multiple signals and/or transcription factors, raises the question of whether self-organized patterning is subject to any general principles. The study of diverse patterning models, in particular reaction-diffusion models, has suggested that spontaneous pattern formation depends on a combination of local activation and long-range inhibition. Patterned cell aggregation can also be interpreted in this way, with local enhancement occurring through cell attraction toward regions of higher density, and long-range inhibition through cell depletion and/or mechanical forces (see below). In the classic activator-inhibitor model, patterning requires a greater diffusivity of the inhibitor (Box 1), and in a model where a nondiffusing species induces a diffusing activator and a diffusing inhibitor, the diffusion range of the inhibitor must be larger (Box 2). But whether local activation and long-range inhibition are always required, in Turing or other models, remains unclear, and has been called into question by a recent study of patterning in reaction-diffusion models. Marcon et al. (2016) conducted a numerical screen for network topologies that can form Turing patterns. In addition to networks where patterning depends on the diffusion parameters, as one might expect, the screen also identified networks where patterning is independent of the diffusion rates. All that can be said about networks that pattern, Marcon et al. (2016) suggest, is that diffusion shifts the balance between stabilizing and destabilizing feedbacks. Still, one could make the case that the behavior of some of the networks identified as independent of the diffusion rates is compatible with the classic interpretation. In one such example, a nondiffusing species induces a diffusing activator, which in turn induces a diffusing inhibitor (see Box 2). Here, the effective range of inhibition compounds the diffusion of activator and inhibitor, thereby exceeding the range of activation regardless of diffusion rates. A more systematic investigation may clarify whether the patterning behavior of arbitrary networks can be understood along the same lines, or whether some follow an inherently different logic.

As a possible entry into this question, generalizing on the previous example, one can introduce an "interaction function" that describes how the state of a cell varies according to the states of surrounding cells (see Box 2). The above-mentioned model for bristle patterning in flies (Corson et al., 2017), which treats signaling as instantaneous, assumes such a structure from the start. For a reaction-diffusion model, an interaction function is most naturally defined when a separation can be made between variables corresponding to an internal "cell state", and to diffusing signals, as in the digit model of (Raspopovic et al., 2014). Of note, such a separation is absent in the classic activator-inhibitor model. And more broadly, it may not be operative if one allows positive feedback among diffusing species, since patterning may then occur without changes in cell state. But when cells interact through diffusing substances that are produced in a cell-state-dependent manner, it is possible to ascribe a signaling field to each cell, and therefore to define an interaction function that couples the cell states. And in that case, it seems reasonable to conjecture that patterning should depend on a distance-dependent balance between activation and inhibition. Beyond reaction-diffusion models, the notion of interaction function may provide a common framework to analyze different interaction modalities, whether chemical and/or mechanical, and abstract, to some degree, the dynamics of pattern formation from the specifics of interaction networks.

Integrating Mechanics with Signaling: Feather and Hair Patterning in Amniotes

To date, most investigations of self-organized patterning have focused on the action of molecular signals. Yet models involving cell migration and/or mechanical forces can give rise to similar patterns, such as spots in two dimensions, and there are multiple instances where they have been proposed as plausible alternatives to chemical models, as in the patterning of digits, as well as feathers and hair (Murray et al., 1983). These skin structures, which cover the body surface of birds and mammals, develop from follicles that form at regular intervals during organogenesis (Figure 3A) and a Turing-like mechanism has long been proposed to explain their arrangement (Nagorcka and Mooney, 1985, 1982). Recent studies in chick and mice have shed new light into the molecular and cellular underpinnings of this patterning process (Glover et al., 2017; Shyer et al., 2017) and on the relative contributions of chemical signals and mechanical forces.

The formation of follicles involves communication between two layers of skin cells that are separated by a basement membrane: the dermis, composed of mesenchymal cells, and the overlying epidermis, a sheet of epithelial cells. At midembryogenesis, cells reorganize to form regularly spaced dermal condensates, i.e., multicellular aggregates of mesenchymal cells in the dermis, associated with closely packed epidermal cells forming placodes. These morphological changes are accompanied by changes in gene expression in both skin layers. Experiments in which the epidermis and dermis from different body parts were separated and recombined suggested that patterning first occurs in the dermis and that patterning information is then relayed to the overlying epidermis (Dhouailly, 1975).

Two types of models have been considered to explain how a pattern emerges in the dermis, and how it is possibly integrated with pattern formation mechanisms operating in the epidermis (Painter et al., 2012). In one, a molecular pattern of gene

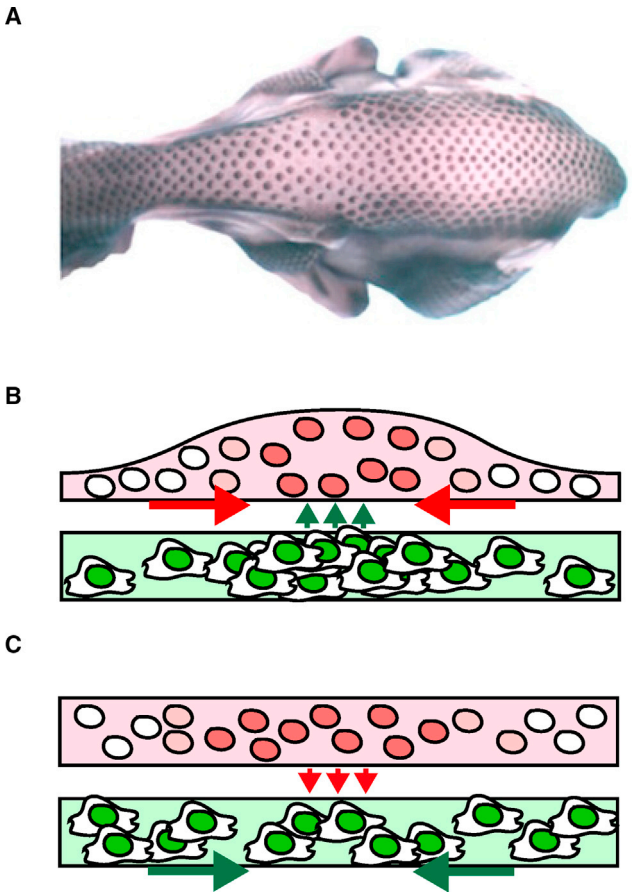

Figure 3. Coupling between Gene Expression Patterning and Mechanics in Feather and Hair Patterning

(A) The emergence of feather and hair primordia (here, feather buds in a chick embryo from Painter et al. [2012]) is marked by changes in gene expression and tissue morphology.

(B) In chick, it proposed that patterned cell aggregation in the dermis (green), through compression of the epidermis (red), drives gene expression patterning (Shyer et al., 2017).

(C) In mouse, while dermal cells retain the ability to self-organize, this may be normally preceded and driven by gene expression patterning in the epidermis (Glover et al., 2017).

expression emerges first, presumably in the dermis, and secondarily directs changes in tissue organization to produce the follicles. Here, patterning has a chemical basis, possibly involving a Turing system. In a second model, mobile mesenchymal cells first organize into regularly spaced aggregates in the dermis, and this pattern of cell aggregates then induces changes in gene expression in both skin layers.

So far, most studies have addressed the first type of model and focused on the identification of the relevant diffusive signals operating as activator-inhibitor pairs, such as Wnt/Dkk in the mouse (Sick et al., 2006) and BMP7/BMP2 in the chick (Michon et al., 2008). There is reason to doubt, however, that any pair of signals can account for skin patterning. Indeed, Shh and FGF are also implicated as activators in the chick and a recent study that examined the interactions between BMP, FGF, and Wnt in the mouse, suggests that positive feedback may occur only indirectly, through multiple inhibitory interactions (Glover et al., 2017). Thus, the precise function of diffusible signals in skin patterning remains unclear. Could it be instead that mechanical cues are the main driver of skin patterning? Since Wnt/β-catenin is active and required in both the dermis and epidermis for skin patterning in mice (Chen et al., 2012; Zhang et al., 2009), and since nuclear β-catenin is a known readout of mechanical cues (Benham-Pyle et al., 2015), it is conceivable that mechanical interactions between contractile mesenchymal cells drive the spontaneous formation of cell aggregates in the dermis and that these dermal aggregates in turn provide an endogenous source of compression for the epidermis. Consistent with this, a recent study in chick indicated that nuclear accumulation of β-catenin did not precede the formation of dermal condensates and epidermal placodes, and the loss of nuclear β-catenin in drug-treated explants did not prevent the formation of multicellular aggregates (Shyer et al., 2017). Also, while untreated explants developed regularly spaced follicles, skin explants under compression (enhanced actomyosin contractility) showed uniform nuclear β-catenin and broad expression of follicle-specific genes. Conversely, nuclear β-catenin and follicle-specific gene expression were lost in relaxed explants (under reduced actomyosin contractility). The formation of condensations was also sensitive to the stiffness of the substrate on which the explants were grown, suggesting that they arise through a mechanical instability that only operates in a certain range of mechanical parameters. The precise nature of this instability remains to be clarified, likely requiring further experimental studies that directly probe mechanical forces within the tissue or compare the effect of substrate stiffness with the application of forces at the tissue border, combined with modeling of force generation and transmission in this layered system. Nevertheless, these results support a model where mobile mesenchymal cells first form a periodic pattern of cell aggregates and this patterning information is then relayed to the epidermis through dermis-induced compressive forces (Figure 3B). Thus, in the chick, mechanical forces are proposed to drive the patterning of feather follicles, and nuclear β-catenin integrates mechanical cues to regulate gene expression in emerging follicles (Shyer et al., 2017).

Is the same process involved in hair formation in the mouse? A recent study suggests that patterning in the epidermis actually precedes the detection of cell aggregates in the dermis, implying that the latter may not pattern the epidermis as in the chick (Glover et al., 2017). Rather, mesenchymal cells may respond to epidermal patterning cues to form dermal condensates in the mouse. Nevertheless, when epidermal patterning is disrupted, as monitored by the loss of nuclear β-catenin activity under BMP inhibition and high FGF, a regular pattern of dermal condensates is observed. Thus, patterning can take place in the dermis in the absence of patterning cues from the epidermis, possibly through self-organized aggregation of mesenchymal as in the chick, although it may normally be driven by a combination of diffusive signals operating in the epidermis (Figure 3C) (Glover et al., 2017). Therefore, self-organized cell aggregation (in the dermis) and reaction-diffusion (in the epidermis) may converge for hair patterning in the mouse. Interestingly, these two mechanisms make different predictions about the positioning of follicles at tissue boundaries (Glover et al., 2017). Indeed, any mechanism based on cell aggregation is fueled by mobile cells migrating toward the emerging condensates; since

the supply of mobile cells is limited next to the edge of the tissue, condensates are predicted to form at a distance from the edge. By contrast, in reaction-diffusion systems based on local activators and long-range inhibitors, the edge serves as a sink for diffusible signaling molecules, hence favoring local activation over long-range inhibition so that follicles will tend to form along tissue boundaries. These predictions were tested by introducing a cut edge in skin explants and by examining the position of dermal condensates relative to the cut edge (Glover et al., 2017). In control explants, cell aggregates were found along the edge, consistent with patterning by diffusible signals. On the other hand, when explants were treated with BMP inhibitors and FGF to inhibit patterning in the epidermis, condensates formed away from the edge, consistent with a driving role for cell aggregation. It thus appears that the ability of dermal cells to self-organize is conserved in amniotes but, in the mouse, is slaved to patterning in the epidermis (Glover et al., 2017).

Further elaborating on the interactions between dermis and epidermis in skin patterning, a recent study in chick has identified FGF expressed in the epidermis as an attractant for dermal cell aggregation (Ho et al., 2019). FGF expression was enhanced upon tissue compression, suggesting that mechanical feedback on gene expression in the epidermis is an integral part of dermal condensate patterning in chick (while mesenchymal transforming growth factor β signaling may support autonomous aggregation in mouse [Glover et al., 2017]). This study also implicated a "priming wave" of ectodysplasin A (EDA) signaling and a tissue-wide gradient of cell density in the sequential formation of the pattern, which is initiated at the dorsal midline and progresses outwards. Specifically, experiments in which EDA signaling and/or cell density were perturbed, combined with a mathematical model introduced by Painter et al. (2018), indicated that EDA modulates a critical cell density above which aggregation can occur, such that the spread of EDA activity, together with a time-dependent profile of cell density, control the timing of follicle formation. The sequential emergence of follicles is essential to produce a regular arrangement, and this was lost when follicle formation was decoupled from the priming wave. As with patterning in the *Drosophila* eye (Lubensky et al., 2011; Roignant and Treisman, 2009), this is an instance where local self-organization, combined with a wave that directs sequential patterning, results in tissue-wide spatial order.

The patterning of hair and feathers nicely illustrates how self-driven morphogenesis and self-patterning (Sasai, 2013) may combine to produce patterns of cell fates. Indeed, the integration of mechanics with chemical signaling is an emerging theme in pattern formation, e.g., quorum sensing by Yap that sets a threshold for the oscillatory expression of clock genes during somitogenesis (Hubaud et al., 2017); buckling and folding of the gut epithelium (in response to compressive stress resulting from smooth muscles resisting the growth of the gut) creates pockets of mesenchymal cells where Shh concentrates, creating a regular distribution of regions with high Shh (devoid of stem cells, corresponding to the villus tip) and regions of low Shh (enriched in stem cells, corresponding to the crypt) (Shyer et al., 2013, 2015). In this regard, it is interesting to note that several cell-cell signaling pathways, e.g., YAP/TAZ, integrin, and Notch, include mechanosensitive molecules.

Stripe Patterning in Fishes: A Turing-like System Based on Interacting Cells?

Most animals exhibit species-specific pigmentation patterns that may serve for camouflage, sexual communication, or mimicry. Theory has long been used to account for these patterns (Koch and Meinhardt, 1994; Murray, 2003). In a landmark study, Kondo and Asai (Kondo and Asal, 1995) proposed that a reaction-diffusion system can account for the stripe pattern seen in adult angelfish. Specifically, the pattern changes recorded over a 2-month period of body growth, including the intercalation of new stripes, matched computer simulations based on a reaction-diffusion model relying on short-range activation and long-range inhibition (although the model was simulated in 1D, and may therefore not support the same sequence in 2D [Höfer and Maini, 1996]). These observations prompted the search for the underlying fast-diffusing inhibitor and slow-diffusing activator, and zebrafish was chosen as a model organism to decipher the molecular and developmental basis of stripe formation. The ensuing studies have provided further support for self-organized patterning, like the observation that, following a local erasure of the stripes, a labyrinthine pattern regenerates and neighboring stripes can be displaced, as predicted by a Turing model (Nakamasu et al., 2009; Yamaguchi et al., 2007). All the while, they have revealed that it involves a much richer repertoire of cell-cell interactions than the simple diffusion of signaling molecules.

The zebrafish owes its name to a series of longitudinal blue and yellow stripes in the trunk and in the fins (Figure 4A). These stripes are produced by the multilayered arrangement of three types of cells present in the skin, the yellow xanthophores, the blue or silvery iridophores, and the black melanophores. Patterning has been best studied in the trunk where the stripe pattern develops in two separate stages. First, a simple pattern of four stripes of black melanophores forms through the migration of neural crest-derived cells during embryogenesis (Singh et al., 2016; Singh and Nüsslein-Volhard, 2015). Iridophores appear to be associated with melanophores, whereas xanthophores are mostly scattered. This larval pattern is essentially complete after six days of development. Second, the adult pattern develops over a one-month period starting three weeks after fertilization. It is in part contributed by the larval xanthophores, which first dedifferentiate and proliferate to cover the trunk as a top layer and then redifferentiate to contribute to the light stripes while remaining undifferentiated in the dark stripe regions. By contrast, the larval iridophores and melanophores do not contribute to the adult pattern. New iridophores and melanophores are produced during metamorphosis by neural crest-derived stem cells that are located deep inside the body (Mahalwar et al., 2014; McMenamin et al., 2014). These iridophores and melanophores (or their immediate precursors) migrate via specific routes toward a skin territory that is largely covered by the yellow xanthophores. Once in the skin, iridophores continue to proliferate whereas melanophores gradually stop dividing and enlarge (Mahalwar et al., 2014; Singh et al., 2016; Singh and Nüsslein-Volhard, 2015).

How then do the yellow (or light) and blue (or dark) stripes emerge? A simplified view, synthesizing a large body of elegant lineage and mutant studies, is presented here (Figure 4B) (Singh and Nüsslein-Volhard, 2015). The first horizontal yellow stripe is

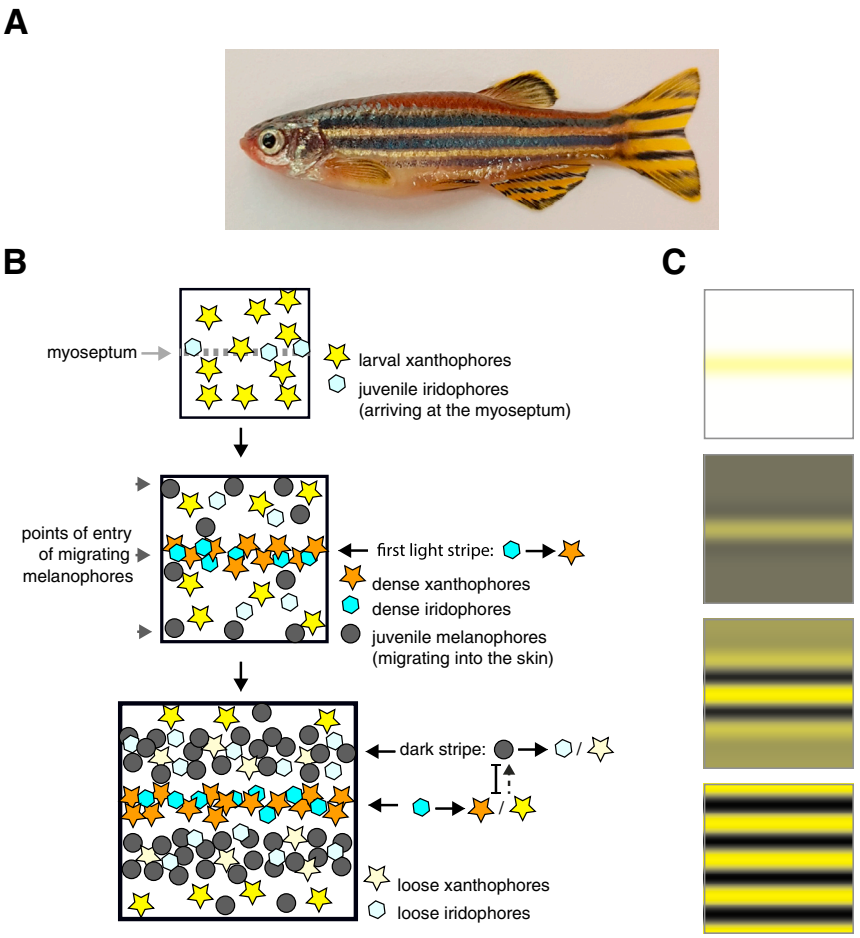

Figure 4. Stripe Patterning through Interactions between Pigment-Carrying Cells in Zebrafish

(A) The stripe pattern in an adult zebrafish (image courtesy of Laure Bally-Cuif).

(B) Schematic of cell-cell interactions involved in stripe patterning. The first light stripe forms through the interaction between iridophores reaching the skin at the myoseptum and xanthophores. Interactions between xanthophores and melanophores, which are inhibitory at short range and activating at long range (dotted arrow), give rise to the adjacent dark stripes (after Singh and Nüsslein-Volhard [2015]).

(C) A Turing-like model based on the interactions between xanthophores (yellow) and melanophores (black), with an initial template comprised of one central stripe, produces a sequence of stripes that progresses outwards from the midline (after Nakamasu et al. [2009]).

organized by iridophores that reach the skin along the myoseptum and interact with the overlying xanthophores to promote the production of the yellow pigments. Next, melanophores preferentially reach the skin along the sides of this first stripe, where they interact with iridophores, which disperse, and xanthophores, which adopt a stellate shape and appear faint. As a result, two blue (or dark) stripes appear flanking the central yellow stripe. Then, as the juvenile fish grow, additional light stripes form through patterned aggregation of iridophores as they delaminate from the light stripes, proliferate, disperse, and reaggregate. The horizontal myoseptum thus seems to serve as a positional cue that orients the stripe pattern as it defines where iridophores first aggregate (Singh and Nüsslein-Volhard, 2015). Consistent with this, mutants lacking the myoseptum exhibit a labyrinthine pattern of stripes with no predominant orientation but normal width (Frohnhöfer et al., 2013). On the other hand, what defines the width of yellow stripes and what triggers iridophores to condense to form the flanking yellow stripes, hence defining the width of the black stripes, is not well understood. Cell-cell interactions are clearly important as revealed by mutant analysis (reviewed in Singh and Nüsslein-Volhard, 2015; Watanabe and Kondo, 2015a). Mutants lacking any one of the three types of pigment cells show strong patterning defects, indicating that no single type is indispensable for patterning per se and that all three cell types contribute to patterning. The analysis of double mutants, in which only one cell type remains, indicates that each type of pigment cell has the ability to cover the entire field (Frohnhöfer et al., 2013). This excludes the possibility that pigment cells interpret a fixed prepattern and instead suggests that patterning involves mutual inhibitory cell-cell interactions. The nature of these interactions has been studied *in vivo*, using laser ablation (Nakamasu et al., 2009), mutant mosaic analysis (Maderspacher and Nüsslein-Volhard, 2003), altered gene expression (Patterson et al., 2014) and conditional inactivation (Parichy and Turner, 2003), as well as *in vitro* (Inaba et al., 2012). Together, these studies indicate that iridophores attract xanthophores and promote their differentiation, and that iridophores and xanthophores repel melanophores at short range and/or promote their death. Melanophores may be further cleared from the yellow stripes through long-distance signaling via cellular projections produced by undifferentiated xanthophore cells located within the black stripes (Eom et al., 2015; Eom and Parichy, 2017), while projections extending from melanophores to xanthophores have been proposed to support melanophore survival and govern the width of the black stripes (Hamada et al., 2014)—although the latter projections may be more prevalent in the adult (Eom et al., 2015). Finally, iridophores promote melanophore survival via a yet unknown mechanism (Frohnhöfer et al., 2013). In summary, long- and short-range cell-cell interactions impacting on cell proliferation (iridophores and xanthophores), cell dispersal (iridophores), survival and differentiation (all cells) appear to form the basis of a self-organized patterning process. Positional cues, provided notably by the myoseptum, may impinge on this self-organized process by specifying the sites where new cells are inserted, resulting in a reproducible outcome.

These developmental studies therefore clearly establish that stripe patterning does not involve a simple reaction-diffusion system with a fast-diffusing inhibitor and slow-diffusing activator

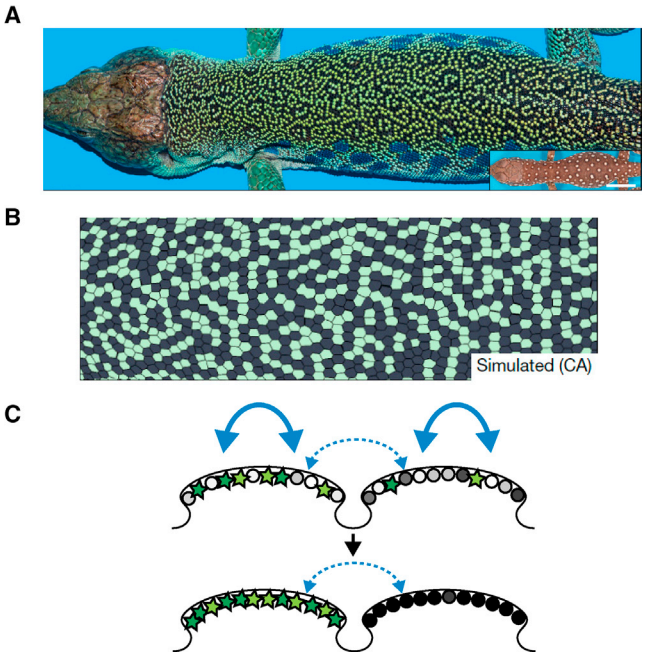

Figure 5. A Multiscale Model for Skin Color Patterning in Lizards
(A) Adult ocellated lizards exhibit a labyrinthine skin pattern, comprised of green and black scales.
(B) A cellular automaton model, in which individual scales switch color according to the states of their neighbors, produces statistically similar patterns.
(C) Interactions between pigmented-carrying cells could account for both the adoption of a single color within each scale, and, acting more weakly through scale borders (dotted arrows), the interactions between scales that drive tissue-wide patterning. A and B from Manukyan et al. (2017).

produced by static and equipotent cells. Actually, any model based on a stripe versus interstripe fate choice taken by immobile and equivalent cells would not be relevant since the elements of the pattern, i.e., the three types of pigment cells, are mobile and display cell-type specific behaviors. In other words, the reaction-diffusion system that was initially proposed (Kondo and Asal, 1995) does not have simple molecular correlates (see [Singh et al., 2015] for discussion), and is best interpreted as an effective description of interacting cell populations. This was made explicit in a later model, with three variables for the densities of melanophores and xantophores, and a signal mediating their interactions (Nakamasu et al., 2009). The model retains the mathematical form of a Turing model, with diffusion substituting for interactions between distant cells. Such a model can recapitulate, qualitatively at least, the sequential emergence of stripes from an initial template (Figure 4C), and the regeneration of a disordered pattern following the laser ablation of skin cells (Nakamasu et al., 2009). And a parallel could be drawn between the amplification of small perturbations in the model, resulting from mutual inhibition between the two cell types, and the "priority effect" whereby the earliest pigment cells to differentiate at a given location influence the makeup of the cell population at later times (Patterson et al., 2014). However, because the key role of iridophores in stripe patterning, and the complexity of the relevant cellular behaviors (proliferation and dispersal, elimination, survival and differentiation to cover a large area, or extend long cytoplasmic processes) remain hidden, the relevance and predictive value of Turing-like models have been disputed (Mahalwar et al., 2014; Singh et al., 2015; Watanabe and Kondo, 2015b). Recently, a model that explicitly incorporates the three cell types has been proposed (Volkening and Sandstede, 2018). This model involves both short- and long-range interactions governing a set of behaviors (death, change in morphology) for all three cell types. Simulations of these discrete-time rules on a mixed population of cells that divide, migrate, and interact in an expanding 2D field were used to suggest that iridophores contributes to patterning robustness (Volkening and Sandstede, 2018). More generally, models that explicitly incorporate the three cell types can readily be compared with a broader set of experimental observations, e.g., patterning dynamics in mutants with only one or two pigment cell types present (Frohnhöfer et al., 2013), and could help clarify the extent to which complex cellular interactions can be reduced to a simpler, effective description, at least in wild type. In addition, the picture that emerged from studies in zebrafish, where positional cues steer a self-organized system toward a defined outcome, could be challenged by studies in other species. Within the genus *Danio* alone, only zebrafish show continuous, longitudinal stripes, which can be traced to the horizontal myoseptum. Other species exhibit diverse patterns, e.g., vertical stripes (Singh and Nüsslein-Volhard, 2015), suggesting that alternative directional cues may be at play.

Evolving Skin Pigmentation Patterns in Lizards: A Cellular Automaton Emerging from Reaction-Diffusion Systems

The systems covered so far emphasize individual cells as the elementary units of tissue patterning. A recent study of skin patterning in lizards, by contrast, suggests an instance where patterning is best understood as the product of interactions between supracellular units. In ocellated lizards, the skin color pattern seen at birth evolves during the life of the animal. In juveniles, regularly spaced white ocelli are observed over a brown background, with each ocellus comprising a dozen of scales. This pattern gradually changes over a three-year period to form a labyrinth-like pattern with about two-thirds of the scales, initially white or brown, becoming black and the remaining third becoming green (Figure 5A). During this process, about a third of the scales individually switch color, from green to black or black to green; these color changes are not random but rather tend to create strings of green or black scales, producing a pattern resembling a labyrinth (Manukyan et al., 2017). This remarkable observation begs two questions: first, how is color determined at the level of individual scales? Each scale is produced by a dermal condensation that comprises pigment-containing chromatophores and light-interfering iridophores. Although the molecular basis of scale color specification is not well understood, it likely involves interactions between structural and pigmentary colors (Saenko et al., 2013). In analogy with the reaction-diffusion system proposed for stripe patterning in fishes, it is proposed that a reaction-diffusion system might regulate the adoption of a single color by a given scale through nonlinear interactions between chromatophores and iridophores. Second, how does a scale switch color as a function of the state of its neighbors? Manukyan et al. (2017) showed that the dynamics of the pattern could be captured by a

probabilistic cellular automaton, where each element (scale) admits a discrete state (color) (Figure 5B). At every time step, the probability that a scale switches color is a function of its current state and the states of its neighbors. Iterated application of this rule, using the experimentally observed switching probabilities, produced patterns that were statistically similar to patterns in the adult. Tying together the cellular and supracellular spatial scales, Manukyan et al. (2017) further proposed that the same cell-cell interactions that lead to a uniform color within scales could account for the coupling between scales, if they act—although more weakly—across scale boundaries (Figure 5C). Indeed, simulations of a reaction-diffusion model with reduced diffusivity at scale borders reproduced the behavior of the cellular automaton made of skin scales. Thus, a single self-organized process may operate at two spatial length scales that are set by a morphological boundary affecting cell-cell interactions, to form a discrete pattern on a supracellular scale.

Perspectives

As illustrated in this review, the study of diverse model systems provides unambiguous evidence for self-organization in tissue patterning and the relevant interactions are now well enough characterized that quantitative comparisons with mathematical models are becoming possible; in addition to interactions mediated by chemical signals, evidence for a role of mechanical forces is accumulating, which should stimulate a re-examination of mechanical models for patterning. All the while, it also evident that multiple, possibly redundant interactions are at play in any given system. And because alternative models centered on different interactions (different combinations of signals, or mechanical forces versus signals) can produce similar patterns, whether we have reached a predictive understanding of pattern formation in these systems is unclear. In particular, it could be said that a definitive example of a Turing system in development remains elusive.

How then can we ascertain our understanding of self-organized patterning? Part of the answer will come from further quantitative experiments that monitor the dynamics of patterning and put models to more stringent tests, such as controlled space- or time-dependent perturbations, using e.g., optogenetic and microfluidic tools (Duncombe et al., 2015; Guglielmi et al., 2016; Tischer and Weiner, 2014). But what we consider a satisfactory model also merits consideration. Detailed models can be difficult to define with confidence and falsify and may not provide the most transparent representation of the underlying "logic". Maybe one should envision a hierarchy of models, incorporating different levels of detail, and embodying different levels of understanding. At the coarsest scale are models that describe pattern formation in the form of geometric rules, such as have been proposed to account for spacing of hair follicles in mouse (Cheng et al., 2014), or, in the context of self-organized morphogenesis, the branching of epithelial structures (Hannezo et al., 2017). Such models, while agnostic about mechanism, are readily confronted with quantitative data: where is the next follicle formed, in wild-type or perturbed conditions? How are intervals between heterocysts distributed in *Anabeana*? And they could be used to constrain finer models. Closer to a dynamic picture are models in which interacting elements (typically cells, but lizard scales are a supracellular example) are endowed with a phenomenological "internal state" and coupled through an interaction function (Corson and Siggia, 2017; François and Siggia, 2012). For instance, one might seek to describe limb or stripe patterning with a single state variable, capturing the digit versus interdigit or stripe versus interstripe decision. In these terms, it might be possible to identify conditions on cell-cell interactions that are required to recapitulate patterning, independent of how they are realized molecularly. Such a description could be challenged by monitoring patterning under aberrant boundary conditions, e.g., altered growth of the limb, or following perturbations that are localized in space or time. Ultimately, live imaging of gene expression and signaling activity, in both wild-type and perturbed conditions, combined with genetic and molecular studies, should make it possible to tie more explicitly the dynamics of fate specification to networks of molecular interactions. A convenient setting for this may be reconstituted *in vitro* systems, such as have been established to study the self-organization of the early mammalian embryo (Etoc et al., 2016). By combining singe-cell RNA sequencing with computational approaches, it is also now possible to identify transitional cell states and to uncover developmental trajectory of heterogenous cell populations in the embryo (Briggs et al., 2018; Farrell et al., 2018; Wagner et al., 2018). These emerging approaches, possibly coupled with lineage tracing based on DNA bar codes (Fletcher et al., 2018; Raj et al., 2018; Wagner et al., 2018), will be useful to study fate dynamics during patterning, as illustrated by the recent identification of dermal condensate precursors during the patterning of the hair follicles in the mouse (Gupta et al., 2019; Mok et al., 2019). Finally, experimental progress in the dissection of mechanical forces acting within tissues should clarify their function in patterning.

In a developing embryo, self-organization never operates in isolation. Boundary conditions, defined by the geometry of a tissue, extrinsic mechanical forces or pre-existing biases (developmental history), may steer patterning toward a defined outcome, or define the initial breaking of symmetry. Likely equally relevant in defining boundary conditions are the temporal cues that define both the onset and the pace of self-organized processes, but these remain largely unexplored, as is the temporal coordination of patterning with other developmental processes in the embryo. More broadly, rather than simply upstream of one another, positional cues and self-organization may be interlinked (Green and Sharpe, 2015), as in bristle patterning where both operate through Delta (Corson et al., 2017). The interplay between multiple, overlapping patterning processes may participate in a reliable outcome. The precision and robustness of development, once theoretical or speculative considerations, can now be approached quantitatively in experiments. Where patterning is directed by positional cues, information theory provides a framework to analyze variability in gene expression, as in the *Drosophila* segmentation hierarchy, downstream of maternal gradients (Dubuis et al., 2013; Petkova et al., 2019). Whether the same concepts carry over to patterns that are refined through cell-cell interactions, or self-organized, remains to be explored. And may require that we embrace the suggestion that information is elaborated, rather than simply read out, during development (Oyama, 2000).

ACKNOWLEDGMENTS

We thank Vincent Hakim and Robert Kelsh for comments on the manuscript. Our work is funded by a collaborative Agence Nationale de la Recherche (ANR) grant (ANR16-CE13-0003-02).

REFERENCES

Akiyama, H., Chaboissier, M.C., Martin, J.F., Schedl, A., and de Crombrugghe, B. (2002). The transcription factor Sox9 has essential roles in successive steps of the chondrocyte differentiation pathway and is required for expression of Sox5 and Sox6. Genes Dev. *16*, 2813–2828.

Akiyama, T., and Gibson, M.C. (2015). Morphogen transport: theoretical and experimental controversies. Wiley Interdiscip. Rev. Dev. Biol. *4*, 99–112.

Amari, S.-I. (1977). Dynamics of pattern formation in lateral-inhibition type neural fields. Biol. Cybern. *27*, 77–87.

Barad, O., Rosin, D., Hornstein, E., and Barkai, N. (2010). Error minimization in lateral inhibition circuits. Sci. Signal. *3*, ra51.

Beccari, L., Moris, N., Girgin, M., Turner, D.A., Baillie-Johnson, P., Cossy, A.C., Lutolf, M.P., Duboule, D., and Arias, A.M. (2018). Multi-axial self-organization properties of mouse embryonic stem cells into gastruloids. Nature *562*, 272–276.

Benham-Pyle, B.W., Pruitt, B.L., and Nelson, W.J. (2015). Cell adhesion. Mechanical strain induces E-cadherin-dependent Yap1 and β-catenin activation to drive cell cycle entry. Science *348*, 1024–1027.

Bhatia, N., and Heisler, M.G. (2018). Self-organizing periodicity in development: organ positioning in plants. Development *145*, dev149336.

Briggs, J.A., Weinreb, C., Wagner, D.E., Megason, S., Peshkin, L., Kirschner, M.W., and Klein, A.M. (2018). The dynamics of gene expression in vertebrate embryogenesis at single-cell resolution. Science *360*, eaar5780.

Brown, A.I., and Rutenberg, A.D. (2014). A storage-based model of heterocyst commitment and patterning in cyanobacteria. Phys. Biol. *11*, 016001.

Campuzano, S., and Modolell, J. (1992). Patterning of the Drosophila nervous system: the achaete-scute gene complex. Trends Genet. *8*, 202–208.

Chen, D., Jarrell, A., Guo, C., Lang, R., and Atit, R. (2012). Dermal β-catenin activity in response to epidermal Wnt ligands is required for fibroblast proliferation and hair follicle initiation. Development *139*, 1522–1533.

Cheng, C.W., Niu, B., Warren, M., Pevny, L.H., Lovell-Badge, R., Hwa, T., and Cheah, K.S.E. (2014). Predicting the spatiotemporal dynamics of hair follicle patterns in the developing mouse. Proc. Natl. Acad. Sci. USA *111*, 2596–2601.

Cohen, M., Georgiou, M., Stevenson, N.L., Miodownik, M., and Baum, B. (2010). Dynamic filopodia transmit intermittent Delta-Notch signaling to drive pattern refinement during lateral inhibition. Dev. Cell *19*, 78–89.

Collier, J.R., Monk, N.A.M., Maini, P.K., and Lewis, J.H. (1996). Pattern formation by lateral inhibition with feedback: a mathematical model of Delta-Notch intercellular signalling. J. Theor. Biol. *183*, 429–446.

Cooper, K.L. (2015). Self-organization in the limb: a Turing mechanism for digit development. Curr. Opin. Genet. Dev. *32*, 92–97.

Corrales-Guerrero, L., Mariscal, V., Flores, E., and Herrero, A. (2013). Functional dissection and evidence for intercellular transfer of the heterocyst-differentiation PatS morphogen. Mol. Microbiol. *88*, 1093–1105.

Corrales-Guerrero, L., Tal, A., Arbel-Goren, R., Mariscal, V., Flores, E., Herrero, A., and Stavans, J. (2015). Spatial fluctuations in expression of the heterocyst differentiation regulatory gene hetR in Anabaena filaments. PLoS Genet. *11*, e1005031.

Corson, F., Couturier, L., Rouault, H., Mazouni, K., and Schweisguth, F. (2017). Self-organized Notch dynamics generate stereotyped sensory organ patterns in Drosophila. Science *356*, eaai7407.

Corson, F., and Siggia, E.D. (2017). Gene-free methodology for cell fate dynamics during development. Elife *6*.

Cotterell, J., Robert-Moreno, A., and Sharpe, J. (2015). A local, self-organizing reaction-diffusion model can explain somite patterning in embryos. Cell Syst. *1*, 257–269.

Crampin, E.J., Gaffney, E.A., and Maini, P.K. (1999). Reaction and diffusion on growing domains: scenarios for robust pattern formation. Bull. Math. Biol. *61*, 1093–1120.

Cross, M., and Greenside, H. (2009). Pattern Formation and Dynamics in Nonequilibrium Systems (Cambridge Univeristy Press).

De Joussineau, C., Soulé, J., Martin, M., Anguille, C., Montcourrier, P., and Alexandre, D. (2003). Delta-promoted filopodia mediate long-range lateral inhibition in Drosophila. Nature *426*, 555–559.

del Álamo, D., Rouault, H., and Schweisguth, F. (2011). Mechanism and significance of cis-inhibition in Notch signalling. Curr. Biol. *21*, R40–R47.

Delgado, I., and Torres, M. (2016). Gradients, waves and timers, an overview of limb patterning models. Semin. Cell Dev. Biol. *49*, 109–115.

Delidakis, C., Monastirioti, M., and Magadi, S.S. (2014). E(spl): genetic, developmental, and evolutionary aspects of a group of invertebrate Hes proteins with close ties to Notch signaling. Curr. Top. Dev. Biol. *110*, 217–262.

Dhouailly, D. (1975). Formation of cutaneous appendages in dermo-epidermal recombinations between reptiles, birds and mammals. Wilehm Roux. Arch. Dev. Biol. *177*, 323–340.

Dias, A.S., de Almeida, I., Belmonte, J.M., Glazier, J.A., and Stern, C.D. (2014). Somites without a clock. Science *343*, 791–795.

Dubuis, J.O., Tkacik, G., Wieschaus, E.F., Gregor, T., and Bialek, W. (2013). Positional information, in bits. Proc. Natl. Acad. Sci. USA *110*, 16301–16308.

Duncombe, T.A., Tentori, A.M., and Herr, A.E. (2015). Microfluidics: reframing biological enquiry. Nat. Rev. Mol. Cell Biol. *16*, 554–567.

Economou, A.D., Ohazama, A., Porntaveetus, T., Sharpe, P.T., Kondo, S., Basson, M.A., Gritli-Linde, A., Cobourne, M.T., and Green, J.B.A. (2012). Periodic stripe formation by a Turing mechanism operating at growth zones in the mammalian palate. Nat. Genet. *44*, 348–351.

Eom, D.S., Bain, E.J., Patterson, L.B., Grout, M.E., and Parichy, D.M. (2015). Long-distance communication by specialized cellular projections during pigment pattern development and evolution. Elife *4*.

Eom, D.S., and Parichy, D.M. (2017). A macrophage relay for long-distance signaling during postembryonic tissue remodeling. Science *355*, 1317–1320.

Ermentrout, B. (1991). Stripes or spots? Nonlinear effects in bifurcation of reaction-diffusion equations on the square. Proc. R. Soc. Lond. A *434*, 413–417.

Etoc, F., Metzger, J., Ruzo, A., Kirst, C., Yoney, A., Ozair, M.Z., Brivanlou, A.H., and Siggia, E.D. (2016). A Balance between secreted inhibitors and edge sensing controls gastruloid self-organization. Dev Cell *39*, 302–315.

Fagotto, F. (2014). The cellular basis of tissue separation. Development *141*, 3303–3318.

Farrell, J.A., Wang, Y., Riesenfeld, S.J., Shekhar, K., Regev, A., and Schier, A.F. (2018). Single-cell reconstruction of developmental trajectories during zebrafish embryogenesis. Science *360*, eaar3131.

Fletcher, R.B., Das, D., and Ngai, J. (2018). Creating lineage trajectory maps via integration of single-cell RNA-sequencing and lineage tracing: integrating transgenic lineage tracing and single-cell RNA-sequencing is a robust approach for mapping developmental lineage trajectories and cell fate changes. BioEssays *40*, e1800056.

François, P., and Siggia, E.D. (2012). Phenotypic models of evolution and development: geometry as destiny. Curr. Opin. Genet. Dev. *22*, 627–633.

Frohnhöfer, H.G., Krauss, J., Maischein, H.M., and Nüsslein-Volhard, C. (2013). Iridophores and their interactions with other chromatophores are required for stripe formation in zebrafish. Development *140*, 2997–3007.

Ghysen, A., and Dambly-Chaudière, C. (1989). Genesis of the Drosophila peripheral nervous system. Trends Genet. *5*, 251–255.

Glover, J.D., Wells, K.L., Matthäus, F., Painter, K.J., Ho, W., Riddell, J., Johansson, J.A., Ford, M.J., Jahoda, C.A.B., Klika, V., et al. (2017). Hierarchical patterning modes orchestrate hair follicle morphogenesis. PLoS Biol. *15*, e2002117.

Goehring, N.W., Trong, P.K., Bois, J.S., Chowdhury, D., Nicola, E.M., Hyman, A.A., and Grill, S.W. (2011). Polarization of PAR proteins by advective triggering of a pattern-forming system. Science *334*, 1137–1141.

Gómez-Skarmeta, J.L., Campuzano, S., and Modolell, J. (2003). Half a century of neural prepatterning: the story of a few bristles and many genes. Nat. Rev. Neurosci. *4*, 587–598.

Green, J.B.A., and Sharpe, J. (2015). Positional information and reaction-diffusion: two big ideas in developmental biology combine. Development *142*, 1203–1211.

Gros, J., and Tabin, C.J. (2014). Vertebrate limb bud formation is initiated by localized epithelial-to-mesenchymal transition. Science *343*, 1253–1256.

Guglielmi, G., Falk, H.J., and De Renzis, S. (2016). Optogenetic control of protein function: from intracellular processes to tissue morphogenesis. Trends Cell Biol. *26*, 864–874.

Gupta, K., Levinsohn, J., Linderman, G., Chen, D., Sun, T.Y., Dong, D., Taketo, M.M., Bosenberg, M., Kluger, Y., Choate, K., et al. (2019). Single-cell analysis reveals a hair follicle dermal niche molecular differentiation trajectory that begins prior to morphogenesis. Dev. Cell *48*, 17–31.

Halatek, J., Brauns, F., and Frey, E. (2018). Self-organization principles of intracellular pattern formation. Philos. Trans. R. Soc. Lond. B. Biol. Sci. *373*.

Hamada, H., Watanabe, M., Lau, H.E., Nishida, T., Hasegawa, T., Parichy, D.M., and Kondo, S. (2014). Involvement of Delta/Notch signaling in zebrafish adult pigment stripe patterning. Development *141*, 318–324.

Hannezo, E., Scheele, C.L.G.J., Moad, M., Drogo, N., Heer, R., Sampogna, R.V., van Rheenen, J., and Simons, B.D. (2017). A unifying theory of branching morphogenesis. Cell *171*, 242–255.

Heitzler, P., and Simpson, P. (1991). The choice of cell fate in the epidermis of Drosophila. Cell *64*, 1083–1092.

Hiscock, T.W., and Megason, S.G. (2015). Mathematically guided approaches to distinguish models of periodic patterning. Development *142*, 409–419.

Hiscock, T.W., Tschopp, P., and Tabin, C.J. (2017). On the formation of digits and joints during limb development. Dev. Cell *41*, 459–465.

Ho, W.K.W., Freem, L., Zhao, D., Painter, K.J., Woolley, T.E., Gaffney, E.A., McGrew, M.J., Tzika, A., Milinkovitch, M.C., Schneider, P., et al. (2019). Feather arrays are patterned by interacting signalling and cell density waves. PLoS Biol. *17*, e3000132.

Höfer, T., and Maini, P.K. (1996). Turing patterns in fish skin? Nature *380*, 678.

Hubaud, A., Regev, I., Mahadevan, L., and Pourquié, O. (2017). Excitable dynamics and Yap-dependent mechanical cues drive the segmentation clock. Cell *171*, 668–682.e11.

Inaba, M., Yamanaka, H., and Kondo, S. (2012). Pigment pattern formation by contact-dependent depolarization. Science *335*, 677.

Karp, X., and Greenwald, I. (2003). Post-transcriptional regulation of the E/Daughterless ortholog HLH-2, negative feedback, and birth order bias during the AC/VU decision in C. elegans. Genes Dev. *17*, 3100–3111.

Keller, E.F., and Segel, L.A. (1970). Initiation of slime mold aggregation viewed as an instability. J. Theor. Biol. *26*, 399–415.

Koch, A.J., and Meinhardt, H. (1994). Biological pattern formation: from basic mechanisms to complex structures. Rev. Mod. Phys. *66*, 1481–1507.

Kondo, S., and Asal, R. (1995). A reaction-diffusion wave on the skin of the marine angelfish Pomacanthus. Nature *376*, 765–768.

Kumar, K., Mella-Herrera, R.A., and Golden, J.W. (2010). Cyanobacterial heterocysts. Cold Spring Harb. Perspect. Biol. *2*, a000315.

Lan, Y., Xu, J., and Jiang, R. (2015). Cellular and molecular mechanisms of palatogenesis. Curr. Top. Dev. Biol. *115*, 59–84.

Lu, P., and Werb, Z. (2008). Patterning mechanisms of branched organs. Science *322*, 1506–1509.

Lubensky, D.K., Pennington, M.W., Shraiman, B.I., and Baker, N.E. (2011). A dynamical model of ommatidial crystal formation. Proc. Natl. Acad. Sci. USA *108*, 11145–11150.

Maderspacher, F., and Nüsslein-Volhard, C. (2003). Formation of the adult pigment pattern in zebrafish requires leopard and obelix dependent cell interactions. Development *130*, 3447–3457.

Mahalwar, P., Walderich, B., Singh, A.P., and Nüsslein-Volhard, C. (2014). Local reorganization of xanthophores fine-tunes and colors the striped pattern of zebrafish. Science *345*, 1362–1364.

Manukyan, L., Montandon, S.A., Fofonjka, A., Smirnov, S., and Milinkovitch, M.C. (2017). A living mesoscopic cellular automaton made of skin scales. Nature *544*, 173–179.

Marcon, L., Diego, X., Sharpe, J., and Müller, P. (2016). High-throughput mathematical analysis identifies Turing networks for patterning with equally diffusing signals. Elife *5*, 1309.

McCauley, H.A., and Wells, J.M. (2017). Pluripotent stem cell-derived organoids: using principles of developmental biology to grow human tissues in a dish. Development *144*, 958–962.

McMenamin, S.K., Bain, E.J., McCann, A.E., Patterson, L.B., Eom, D.S., Waller, Z.P., Hamill, J.C., Kuhlman, J.A., Eisen, J.S., and Parichy, D.M. (2014). Thyroid hormone-dependent adult pigment cell lineage and pattern in zebrafish. Science *345*, 1358–1361.

Meeks, J.C., and Elhai, J. (2002). Regulation of cellular differentiation in filamentous cyanobacteria in free-living and plant-associated symbiotic growth states. Microbiol. Mol. Biol. Rev. *66*, 94–121.

Michon, F., Forest, L., Collomb, E., Demongeot, J., and Dhouailly, D. (2008). BMP2 and BMP7 play antagonistic roles in feather induction. Development *135*, 2797–2805.

Mitchison, G.J., and Wilcox, M. (1972). Rule governing cell division in Anabaena. Nature *239*, 110–111.

Miura, T., and Shiota, K. (2000). TGFbeta2 acts as an "activator" molecule in reaction-diffusion model and is involved in cell sorting phenomenon in mouse limb micromass culture. Dev. Dyn. *217*, 241–249.

Mok, K.W., Saxena, N., Heitman, N., Grisanti, L., Srivastava, D., Muraro, M.J., Jacob, T., Sennett, R., Wang, Z., Su, Y., et al. (2019). Dermal condensate niche fate specification occurs prior to formation and is placode progenitor dependent. Dev. Cell *48*, 32–48.

Montesano, R., Schaller, G., and Orci, L. (1991). Induction of epithelial tubular morphogenesis in vitro by fibroblast-derived soluble factors. Cell *66*, 697–711.

Müller, P., Rogers, K.W., Jordan, B.M., Lee, J.S., Robson, D., Ramanathan, S., and Schier, A.F. (2012). Differential diffusivity of Nodal and lefty underlies a reaction-diffusion patterning system. Science *336*, 721–724.

Müller, P., Rogers, K.W., Yu, S.R., Brand, M., and Schier, A.F. (2013). Morphogen transport. Development *140*, 1621–1638.

Muñoz-García, J., and Ares, S. (2016). Formation and maintenance of nitrogen-fixing cell patterns in filamentous cyanobacteria. Proc. Natl. Acad. Sci. USA *113*, 6218–6223.

Murray, J.D. (2003). Mathematical Biology, Third Edition (Springer).

Murray, J.D., Oster, G.F., and Harris, A.K. (1983). A mechanical model for mesenchymal morphogenesis. J. Math. Biol. *17*, 125–129.

Nagorcka, B.N., and Mooney, J.R. (1985). The role of a reaction-diffusion system in the initiation of primary hair follicles. J. Theor. Biol. *114*, 243–272.

Nagorcka, B.N., and Mooney, J.R. (1982). The role of a reaction–diffusion system in the formation of hair fibres. J. Theor. Biol. *98*, 575–607.

Nakamasu, A., Takahashi, G., Kanbe, A., and Kondo, S. (2009). Interactions between zebrafish pigment cells responsible for the generation of Turing patterns. Proc. Natl. Acad. Sci. USA *106*, 8429–8434.

Nakamura, T., Mine, N., Nakaguchi, E., Mochizuki, A., Yamamoto, M., Yashiro, K., Meno, C., and Hamada, H. (2006). Generation of robust left-right asymmetry in the mouse embryo requires a self-enhancement and lateral-inhibition system. Dev. Cell *11*, 495–504.

Newman, S.A., and Frisch, H.L. (1979). Dynamics of skeletal pattern formation in developing chick limb. Science *205*, 662–668.

Ochoa-Espinosa, A., and Affolter, M. (2012). Branching morphogenesis: from cells to organs and back. Cold Spring Harb. Perspect. Biol. *4*, a008243.

Onimaru, K., Marcon, L., Musy, M., Tanaka, M., and Sharpe, J. (2016). The fin-to-limb transition as the re-organization of a Turing pattern. Nat Comms. *7*, 11582.

Oyama, S. (2000). The Ontogeny of Information: Developmental Systems and Evolution (Duke University Press).

Painter, K.J., Ho, W., and Headon, D.J. (2018). A chemotaxis model of feather primordia pattern formation during avian development. J. Theor. Biol. *437*, 225–238.

Painter, K.J., Hunt, G.S., Wells, K.L., Johansson, J.A., and Headon, D.J. (2012). Towards an integrated experimental-theoretical approach for assessing the mechanistic basis of hair and feather morphogenesis. Interface Focus *2*, 433–450.

Parichy, D.M., and Turner, J.M. (2003). Temporal and cellular requirements for Fms signaling during zebrafish adult pigment pattern development. Development *130*, 817–833.

Parks, A.L., Huppert, S.S., and Muskavitch, M.A. (1997). The dynamics of neurogenic signalling underlying bristle development in Drosophila melanogaster. Mech. Dev. *63*, 61–74.

Patterson, L.B., Bain, E.J., and Parichy, D.M. (2014). Pigment cell interactions and differential xanthophore recruitment underlying zebrafish stripe reiteration and Danio pattern evolution. Nat. Comms. *5*, 5299.

Petkova, M.D., Tkačik, G., Bialek, W., Wieschaus, E.F., and Gregor, T. (2019). Optimal decoding of cellular identities in a genetic network. Cell *176*, 844–855.e15.

Plahte, E. (2001). Pattern formation in discrete cell lattices. J. Math. Biol. *43*, 411–445.

Pourquié, O. (2011). Vertebrate segmentation: from cyclic gene networks to scoliosis. Cell *145*, 650–663.

Raj, B., Wagner, D.E., McKenna, A., Pandey, S., Klein, A.M., Shendure, J., Gagnon, J.A., and Schier, A.F. (2018). Simultaneous single-cell profiling of lineages and cell types in the vertebrate brain. Nat. Biotechnol. *36*, 442–450.

Raspopovic, J., Marcon, L., Russo, L., and Sharpe, J. (2014). Modeling digits. Digit patterning is controlled by a Bmp-Sox9-Wnt turing network modulated by morphogen gradients. Science *345*, 566–570.

Ribes, V., and Briscoe, J. (2009). Establishing and interpreting graded sonic hedgehog signaling during vertebrate neural tube patterning: the role of negative feedback. Cold Spring Harb. Perspect. Biol. *1*, a002014.

Risser, D.D., and Callahan, S.M. (2009). Genetic and cytological evidence that heterocyst patterning is regulated by inhibitor gradients that promote activator decay. Proc. Natl. Acad. Sci. USA *106*, 19884–19888.

Risser, D.D., Wong, F.C.Y., and Meeks, J.C. (2012). Biased inheritance of the protein PatN frees vegetative cells to initiate patterned heterocyst differentiation. Proc. Natl. Acad. Sci. USA *109*, 15342–15347.

Rogers, K.W., Lord, N.D., Gagnon, J.A., Pauli, A., Zimmerman, S., Aksel, D.C., Reyon, D., Tsai, S.Q., Joung, J.K., and Schier, A.F. (2017). Nodal patterning without Lefty inhibitory feedback is functional but fragile. Elife *6*, 178.

Roignant, J.Y., and Treisman, J.E. (2009). Pattern formation in the Drosophila eye disc. Int. J. Dev. Biol. *53*, 795–804.

Ros, M.A., Lyons, G.E., Mackem, S., and Fallon, J.F. (1994). Recombinant limbs as a model to study homeobox gene regulation during limb development. Dev. Biol. *166*, 59–72.

Roth, S. (2011). Mathematics and biology: a Kantian view on the history of pattern formation theory. Dev. Genes Evol. *221*, 255–279.

Saenko, S.V., Teyssier, J., van der Marel, D., and Milinkovitch, M.C. (2013). Precise colocalization of interacting structural and pigmentary elements generates extensive color pattern variation in Phelsuma lizards. BMC Biol. *11*, 105.

Sasai, Y. (2013). Cytosystems dynamics in self-organization of tissue architecture. Nature *493*, 318–326.

Sheth, R., Marcon, L., Bastida, M.F., Junco, M., Quintana, L., Dahn, R., Kmita, M., Sharpe, J., and Ros, M.A. (2012). Hox genes regulate digit patterning by controlling the wavelength of a Turing-type mechanism. Science *338*, 1476–1480.

Shyer, A.E., Huycke, T.R., Lee, C., Mahadevan, L., and Tabin, C.J. (2015). Bending gradients: how the intestinal stem cell gets its home. Cell *161*, 569–580.

Shyer, A.E., Rodrigues, A.R., Schroeder, G.G., Kassianidou, E., Kumar, S., and Harland, R.M. (2017). Emergent cellular self-organization and mechanosensation initiate follicle pattern in the avian skin. Science *357*, 811–815.

Shyer, A.E., Tallinen, T., Nerurkar, N.L., Wei, Z., Gil, E.S., Kaplan, D.L., Tabin, C.J., and Mahadevan, L. (2013). Villification: how the gut gets its villi. Science *342*, 212–218.

Sick, S., Reinker, S., Timmer, J., and Schlake, T. (2006). WNT and DKK determine hair follicle spacing through a reaction-diffusion mechanism. Science *314*, 1447–1450.

Simpson, P. (1990). Lateral inhibition and the development of the sensory bristles of the adult peripheral nervous system of Drosophila. Development *109*, 509–519.

Simpson, P., Woehl, R., and Usui, K. (1999). The development and evolution of bristle patterns in Diptera. Development *126*, 1349–1364.

Singh, A.P., Dinwiddie, A., Mahalwar, P., Schach, U., Linker, C., Irion, U., and Nüsslein-Volhard, C. (2016). Pigment cell progenitors in zebrafish remain multipotent through metamorphosis. Dev. Cell *38*, 316–330.

Singh, A.P., Frohnhöfer, H.G., Irion, U., and Nüsslein-Volhard, C. (2015). Fish pigmentation. Response to comment on ''Local reorganization of xanthophores fine-tunes and colors the striped pattern of zebrafish''. Science *348*, 297.

Singh, A.P., and Nüsslein-Volhard, C. (2015). Zebrafish stripes as a model for vertebrate colour pattern formation. Curr. Biol. *25*, R81–R92.

Sonnen, K.F., Lauschke, V.M., Uraji, J., Falk, H.J., Petersen, Y., Funk, M.C., Beaupeux, M., François, P., Merten, C.A., and Aulehla, A. (2018). Modulation of phase shift between Wnt and Notch signaling oscillations controls mesoderm segmentation. Cell *172*, 1079–1090.

Sprinzak, D., Lakhanpal, A., Lebon, L., Garcia-Ojalvo, J., and Elowitz, M.B. (2011). Mutual inactivation of Notch receptors and ligands facilitates developmental patterning. PLoS Comput. Biol. *7*, e1002069.

Stückemann, T., Cleland, J.P., Werner, S., Thi-Kim, V., Bayersdorf, H., Liu, R., Friedrich, S.-Y., Jülicher, B., and Rink, J.C. (2017). Antagonistic self-organizing patterning systems control maintenance and regeneration of the anteroposterior axis in planarians. Dev. Cell *40*, 248–263.e4.

Tischer, D., and Weiner, O.D. (2014). Illuminating cell signalling with optogenetic tools. Nat. Rev. Mol. Cell Biol. *15*, 551–558.

Towers, M., Mahood, R., Yin, Y., and Tickle, C. (2008). Integration of growth and specification in chick wing digit-patterning. Nature *452*, 882–886.

Troost, T., Schneider, M., and Klein, T. (2015). A re-examination of the selection of the sensory organ precursor of the bristle sensilla of Drosophila melanogaster. PLoS Genet. *11*, e1004911.

Tsiairis, C.D., and Aulehla, A. (2016). Self-organization of embryonic genetic oscillators into spatiotemporal wave patterns. Cell *164*, 656–667.

Turing, A.M. (1952). The chemical basis of morphogenesis. Phil. Trans. R. Soc. Lond. B *237*, 37–72.

Turner, D.A., Baillie-Johnson, P., and Martinez Arias, A. (2016). Organoids and the genetically encoded self-assembly of embryonic stem cells. BioEssays *38*, 181–191.

Volkening, A., and Sandstede, B. (2018). Iridophores as a source of robustness in zebrafish stripes and variability in Danio patterns. Nat. Comms. *9*, 3231.

Wagner, D.E., Weinreb, C., Collins, Z.M., Briggs, J.A., Megason, S.G., and Klein, A.M. (2018). Single-cell mapping of gene expression landscapes and lineage in the zebrafish embryo. Science *360*, 981–987.

Warmflash, A., Sorre, B., Etoc, F., Siggia, E.D., and Brivanlou, A.H. (2014). A method to recapitulate early embryonic spatial patterning in human embryonic stem cells. Nat. Methods *11*, 847–854.

Watanabe, M., and Kondo, S. (2015a). Is pigment patterning in fish skin determined by the Turing mechanism? Trends Genet. *31*, 88–96.

Watanabe, M., and Kondo, S. (2015b). Fish pigmentation. Comment on "Local reorganization of xanthophores fine-tunes and colors the striped pattern of zebrafish". Science *348*, 297.

White, M.D., Zenker, J., Bissiere, S., and Plachta, N. (2018). Instructions for assembling the early mammalian embryo. Dev. Cell *45*, 667–679.

Wigglesworth, V.B. (1940). Local and general factors in the development of "pattern" in Rhodnius prolixus (Hemiptera). J. Exp. Biol. *17*, 180–201.

Wilby, O.K., and Ede, D.A. (1975). A model generating the pattern of cartilage skeletal elements in the embryonic chick limb. J. Theor. Biol. *52*, 199–217.

Wilcox, M., Mitchison, G.J., and Smith, R.J. (1973a). Pattern formation in the blue-green alga, Anabaena. I. Basic mechanisms. J. Cell Sci. *12*, 707–723.

Wilcox, M., Mitchison, G.J., and Smith, R.J. (1973b). Pattern formation in the blue-green alga Anabaena. II. Controlled proheterocyst regression. J. Cell Sci. *13*, 637–649.

Wolk, C.P., and Quine, M.P. (1975). Formation of one-dimensional patterns by stochastic processes and by filamentous blue-green algae. Dev. Biol. *46*, 370–382.

Wolpert, L. (1969). Positional information and the spatial pattern of cellular differentiation. J. Theor. Biol. *25*, 1–47.

Yamaguchi, M., Yoshimoto, E., and Kondo, S. (2007). Pattern regulation in the stripe of zebrafish suggests an underlying dynamic and autonomous mechanism. Proc. Natl. Acad. Sci. USA *104*, 4790–4793.

Zhang, Y., Tomann, P., Andl, T., Gallant, N.M., Huelsken, J., Jerchow, B., Birchmeier, W., Paus, R., Piccolo, S., Mikkola, M.L., et al. (2009). Reciprocal requirements for EDA/EDAR/NF-kappaB and Wnt/beta-catenin signaling pathways in hair follicle induction. Dev. Cell *17*, 49–61.

Zhu, J., Nakamura, E., Nguyen, M.T., Bao, X., Akiyama, H., and Mackem, S. (2008). Uncoupling Sonic hedgehog control of pattern and expansion of the developing limb bud. Dev. Cell *14*, 624–632.

Zwilling, E. (1964). Development of fragmented and of dissociated limb bud mesoderm. Dev. Biol. *9*, 20–37.